HHS Public Access

Author manuscript

*Pharmacol Res*. Author manuscript; available in PMC 2023 January 30.

Published in final edited form as:

*Pharmacol Res*. 2021 August ; 170: 105745. doi:10.1016/j.phrs.2021.105745.

# Heteromerization between $\alpha_{2A}$ adrenoceptors and different polymorphic variants of the dopamine $D_4$ receptor determines pharmacological and functional differences. Implications for impulsive-control disorders

**Verònica Casadó-Anguera**[a], **Estefanía Moreno**[a], **Marta Sánchez-Soto**[b,1], **Ning Sheng Cai**[b], **Jordi Bonaventura**[b,c], **Patricia Homar-Ruano**[a], **Marcelo Rubinstein**[d], **Antoni Cortés**[a], **Enric I. Canela**[a], **Sergi Ferré**[b,*], **Vicent Casadó**[a,*]

[a]Department of Biochemistry and Molecular Biomedicine, Faculty of Biology, Institute of Biomedicine of the University of Barcelona (IBUB), University of Barcelona, Barcelona, Spain

[b]Integrative Neurobiology Section, National Institute on Drug Abuse, Intramural Research Program, National Institutes of Health, Baltimore, United States

[c]Biobehavioral Imaging and Molecular Neuropsychopharmacology Unit, National Institute on Drug Abuse, Intramural Research Program, Baltimore, United States

[d]Institute of Investigation in Genetic Engineering and Molecular Biology, Buenos Aires, Argentina

## Abstract

[*]**Corresponding author at:** sferre@intra.nida.nih.gov (SF); vcasado@ub.edu (VC).

[1]**Present address:** Molecular Neuropharmacology Section, National Institute of Neurological Disorders and Stroke Intramural Research Program, Bethesda, United States

Author contributions

V.C.-A., E.M., A.C., E.-I.C., S.F., V.C. participated in the research design. V.C.-A. conducted all the experiments. E.M. aided with BRET, PLA and ERK phosphorylation experiments. M.S.-S. performed and aided with CODA-RET assays. J.B. aided with mice experiments. P.H.-R. aided with BRET experiments. A.C., V.C. aided with binding assays. N.-S.C., M.R. contributed research materials. V.C.-A., E.M., M.S.-S., J.B., S.F., V.C. contributed to the data analyses and interpretation. E.-I.C., S.F., V.C. acquired funding. V.C.-A., E.M., M.S.-S., J.B., M.R., S.F. and V.C. wrote or contributed to the writing and revision of the manuscript. All authors contributed to and have approved the final manuscript.

Supplementary material

Supplementary material related to this article can be found, in the online version.

Chemical compounds studied in this article:

A-412997 dihydrochloride (PubChem CID: 90488953)

BRL 44408 maleate (PubChem CID: 10382026)

Clonidine hydrochloride (PubChem CID: 20179)

Dexmedetomidine hydrochloride (PubChem CID: 6918081)

Guanfacine hydrochloride (PubChem CID: 71401)

L-745,870 trihydrochloride (PubChem CID: 49759035)

Pramipexole dihydrochloride (PubChem CID: 119569)

Ropinirole (PubChem CID: 5095)

Rotigotine hydrochloride (PubChem CID: 180335)

RX 821002 hydrochloride (PubChem CID: 11957683)

Declaration of Competing Interest

The authors declare that no competing interests exist.

Polymorphic alleles of the human dopamine $D_4$ receptor gene (*DRD4*) have been consistently associated with individual differences in personality traits and neuropsychiatric disorders, particularly between the gene encoding dopamine $D_{4.7}$ receptor variant and attention deficit hyperactivity disorder (ADHD). The $\alpha_{2A}$ adrenoceptor gene has also been associated with ADHD. In fact, drugs targeting the $\alpha_{2A}$ adrenoceptor ($\alpha_{2A}R$), such as guanfacine, are commonly used in ADHD treatment. In view of the involvement of dopamine $D_4$ receptor ($D_4R$) and $\alpha_{2A}R$ in ADHD and impulsivity, their concurrent localization in cortical pyramidal neurons and the demonstrated ability of $D_4R$ to form functional heteromers with other G protein-coupled receptors, in this study we evaluate whether the $\alpha_{2A}R$ forms functional heteromers with $D_4R$ and weather these heteromers show different properties depending on the $D_4R$ variant involved. Using cortical brain slices from $hD_{4.7}R$ knock-in and wild-type mice, here, we demonstrate that $\alpha_{2A}R$ and $D_4R$ heteromerize and constitute a significant functional population of cortical $\alpha_{2A}R$ and $D_4R$. Moreover, in cortical slices from wild-type mice and in cells transfected with $\alpha_{2A}R$ and $D_{4.4}R$, we detect a negative crosstalk within the heteromer. This negative crosstalk is lost in cortex from $hD_{4.7}R$ knock-in mice and in cells expressing the $D_{4.7}R$ polymorphic variant. We also show a lack of efficacy of $D_4R$ ligands to promote G protein activation and signaling only within the $\alpha_{2A}R$-$D_{4.7}R$ heteromer. Taken together, our results suggest that $\alpha_{2A}R$-$D_4R$ heteromers play a pivotal role in catecholaminergic signaling in the brain cortex and are likely targets for ADHD pharmacotherapy.

**Keywords**

$\alpha_{2A}$ adrenoceptor; ADHD; cerebral cortex; dopamine $D_4$ receptor; GPCR; receptor heteromer

## 1. Introduction

In recent years, the role of the so-called dopamine $D_4$ receptor ($D_4R$) in the brain is shifting from it being considered a pure dopamine receptor. Several studies indicate that $D_4R$ can indeed respond to other endogenous catecholamines [1–3]. $D_4R$ can be targeted by norepinephrine (NE), and it is able to modulate the function of other catecholamine receptors by heteromerization. Those include pineal $\alpha_{1B}$ and $\beta_1$ adrenoceptors ($\alpha_{1B}R$ and $\beta_1R$, respectively) [4] and striatal dopamine $D_2$ receptors ($D_2R$) [1,5,6]. In addition, heteromerization seems to determine the functional differences of the most frequent products of the *DRD4* gene polymorphisms.

The clearest association between adrenoceptors and $D_4Rs$ occurs in the pineal gland, which contains dense noradrenergic terminals [4,7]. Pinealocytes show a high expression of adrenoceptors of the Gq-coupled $\alpha_{1B}R$ subtype and the Gs-coupled $\beta_1R$ subtype which play a stimulatory role in the synthesis and release of melatonin and its precursor serotonin [8]. In addition, pinealocytes show a marked circadian expression of $D_4R$, decreasing very significantly during daylight and being mostly absent at sunset and maximal at sunrise [7]. It was shown that the main effect of $D_4R$ activation in the pineal gland is to decrease melatonin synthesis and release by inhibiting $\beta_1R$ and $\alpha_{1B}R$ signaling through heteromerization [4].

In the brain, aside from the pineal gland, $D_4R$ are particularly expressed in prefrontal cortical pyramidal glutamatergic neurons, which express $D_4R$ both at the somato-dendritic level and in their striatal terminals [5,6,9–12]. Some studies indicate that, at the terminal level, $D_4R$ form heteromers with $D_2R$ and that these G protein-coupled receptor (GPCR) complexes play a significant inhibitory control of cortico-striatal glutamatergic transmission [5,6].

The human *DRD4* gene displays a high number of polymorphisms in its coding sequence. The most extensive polymorphism is found in exon 3, which is a region that encodes the third intracellular loop (3IL) of the receptor [13–15]. This polymorphism consists of a variable number of tandem repeats of a 48-base pair sequence, with 2 to 11 repeats. The two most common polymorphisms contain 4 and 7 repeats (with allele frequencies of about 60% and 20%, respectively) [14] and they encode a dopamine $D_4R$ with 4 and 7 repeats of a proline-rich sequence of 16 amino acids ($D_{4.4}R$ and $D_{4.7}R$) [13–15]. *DRD4* polymorphisms have been associated with individual differences in personality traits and neuropsychiatric disorders, particularly between the gene encoding $D_{4.7}R$ and attention deficit hyperactivity disorder (ADHD) or substance use disorder (SUD) [13,16–20]. In fact, there is a clear association between $D_{4.7}R$ and impulsivity traits, action impulsivity and choice impulsivity, which are considered endophenotypes of ADHD and SUD [19,21–23].

The question of the functional differences between $D_{4.4}R$ and $D_{4.7}R$ has remained enigmatic until considering GPCR heteromerization. Thus, $D_{4.4}R$ and $D_{4.7}R$ (and other $D_4R$ polymorphic variants) do not show clear functional differences when studied in isolation, but their properties significantly differed when considered as components of $D_2R$-$D_4R$ heteromers [1,3]. The most remarkable functional difference between $D_2R$-$D_{4.4}R$ and $D_2R$-$D_{4.7}R$ was the selective increase in the constitutive activity of $D_2R$ when forming heteromers with $D_{4.7}R$, but not with $D_{4.4}R$ [1]. This gain of function of the $D_2R$-$D_{4.7}R$ heteromer could then explain the increased inhibitory effect of dopamine (DA) on cortico-striatal glutamatergic transmission of mice expressing a $D_4R$ with a humanized 3IL corresponding to the $D_{4.7}R$ [6]. These results suggested that the $D_{4.7}R$-associated increased vulnerability of ADHD and SUD could be related to an enhanced $D_2R$-$D_4R$-mediated dopaminergic control of cortico-striatal transmission.

In addition to the *DRD4* gene, the $\alpha_{2A}$ adrenoceptor ($\alpha_{2A}R$) gene has also been associated with ADHD [24,25]. Although, a large meta-analysis did not find a consistent significant association [18], a more recent study performed at the endophenotype level, established a clear significant association between $\alpha_{2A}R$ gene polymorphisms and action impulsivity [26]. In fact, $\alpha_{2A}R$ localized in pyramidal neurons of the prefrontal cortex [27] are targets of drugs used in the treatment of ADHD such as methylphenidate and the selective $\alpha_{2A}R$ agonist guanfacine [28–30]. In view of the involvement of $D_4R$ and $\alpha_{2A}R$ in impulsivity and ADHD, their concurrent localization in cortical pyramidal neurons and the demonstrated ability of $D_4R$ to form functional heteromers with other adrenoceptors in the pineal gland, we investigated the possibility of $\alpha_{2A}R$-$D_{4.4}R$ and $\alpha_{2A}R$-$D_{4.7}R$ heteromerization in mammalian transfected cells and their localization and functional role in the mouse cerebral cortex.

## 2. Material and methods

### 2.1. DNA constructs

For bimolecular luminescence complementation experiments, human $D_{4.4}R$, $D_{4.7}R$, $\alpha_{2A}R$, $\alpha_{1A}R$, and $A_1R$ were cloned in frame into pcDNA3.1 expressing the amino acid residues 1-229 (nRLuc) or 230-311 (cRLuc) of the RLuc8 protein. For BRET assays, human $D_{4.4}R$-YFP, $D_{4.7}R$-YFP, $\alpha_{1A}R$-YFP, $\alpha_{2A}R$-RLuc8 ($\alpha_{2A}R$-RLuc) and $A_1R$-RLuc constructs were used. For CODA-RET and receptor-G protein BRET assays, the following human G protein constructs were used: $G\alpha_{i1}$-mVenus and $G\alpha_{o1}$-mVenus (with the YFP derivative mVenus inserted at position 91), untagged $G\beta_1$ and $G\gamma_2$ as well as $\alpha_{2A}R$-nRLuc, $\alpha_{2A}R$-cRLuc, $D_{4.4}R$-nRLuc, $D_{4.4}R$-cRLuc, $D_{4.7}R$-nRLuc, $D_{4.7}R$-cRLuc, $D_{4.4}R$, $D_{4.7}R$ and $\alpha_{2A}R$-RLuc and unfused $D_{4.4}R$ and $D_{4.7}R$. For binding and functional assays, $\alpha_{2A}R$-RLuc was used. All the constructs were confirmed by sequencing analysis. Details of key resources used such as cell lines, animal models, reagents and software appear in table S1.

### 2.2. TAT-TM peptides

A peptide derived from the HIV-transactivator of transcription (TAT: YGRKKRRQRRR), was fused to peptides with the amino acid sequences of human $D_4Rs$ or $\alpha_{2A}Rs$ transmembrane (TM) domains 4-7 (Peptide Synthesis Facility, University Pompeu Fabra, Barcelona, Spain), to promote integration of the TM domains in the plasma membrane. Because HIV TAT binds to the phosphatidylinositol-(4, 5)-bisphosphate found on the inner surface of the membrane [31], HIV TAT peptide was fused to the N-terminus of TM4 and TM6 and to the C-terminus of TM5 and TM7 to obtain the right orientation of the inserted peptide. The amino acid sequences were:

TAT-TM4 of D4R: RRRQRRKKRGYGSRRQLLLIGATWLLSAAVAAPVLCGL

TM5-TAT of D4R: YVVYSSVCSFFLPCPLMLLLYWATFYGRKKRRQRRR

TAT-TM6 of D4R: RRRQRRKKRGYAMRVLPVVVGAFLLCWTPFFVVHITQAL

TM7-TAT of D4R: LVSAVTWLGYVNSALNPVIYTVFNAYGRKKRRQRRR

TAT-TM4 of $\alpha_{2A}R$: RRRQRRKKRGYPRRIKAIIITVWVISAVISFPPLI

TM5-TAT of $\alpha_{2A}R$: YKWYVISSCIGSFFAPCLIMILVYVRIYQIAYGRKKRRQRRR

TAT-TM6 of $\alpha_{2A}R$: RRRQRRKKRGYFTFVLAVVIGVFVVCWFPFFFTYTLTAV

TM7-TAT of $\alpha_{2A}R$: RTLFKFFFWFGYCNSSLNPVIYTIFNYGRKKRRQRRR

### 2.3. Cell culture

HEK-293T cells were purchased from ATCC and kept below passage 20. Cells were maintained in culture with Dulbecco's modified Eagle's medium (DMEM) (Gibco™, ThermoFisher Scientific, MA, USA) supplemented with 2 mM L-glutamine, 100 U/mL penicillin/streptomycin, MEM Non-Essential Amino Acid Solution (1/100), and 5% (v/v) heat-inactivated fetal bovine serum 5% fetal bovine serum (all supplements were from

Gibco™, ThermoFisher Scientific) and kept in an incubator at 37°C and 5% $CO_2$. HEK-293T cells inducible expressing $D_4R$ variants under the control of tetracycline, were obtained with the Flp-In T-Rex system. These cell lines were maintained with hygromycin 50 μg/ml and blasticidin 15 μg/ml and the $D_4R$ variant expression was induced for 18-24h with tetracycline 250 ng/ml.

### 2.4. BRET saturation experiments and bimolecular luminescence complementation assays

In order to perform the bioluminescence resonance energy transfer (BRET) assays, cells were transiently co-transfected with polyethylenimine (Sigma, St. Louis, MO, USA) with a constant amount of expression vector encoding for receptor fused to RLuc and with increasing amounts of the expression vector corresponding to receptor fused to YFP (0.55 μg of $\alpha_{2A}R$-RLuc and 0.2-3 μg of $D_{4.4}R$-YFP or 0.2-3.5 μg of $D_{4.7}R$-YFP or 0.2-2 μg of $\alpha_{1A}R$-YFP; 0.1-1 μg of $A_1R$-RLuc, in order to obtain a constant amount of luminescence emission, and 0.1-8 μg of $D_{4.4}R$-YFP. Cells were harvested, washed, and resuspended in PBS. For determining Venus expression, 20 μg of protein were distributed in 96-well plates (black plates with a transparent bottom) and the emission at 530 nm after the excitation at 500 nm with a Mithras LB940 (Berthold Technologies, Bad Wildbad, Germany) was quantified. Protein fluorescence expression was determined as the fluorescence of the sample minus the fluorescence of cells expressing the receptor fused to RLuc alone. In parallel, luminescence and BRET signal was determined as the ratio of the light emitted by Venus (530 nm) over that emitted by coelenterazine H (PJK, Kleinblittersdorf, Germany,) (485 nm) 1 min after the addition of 5 μM coelenterazine H using a Mithras LB940. To quantify receptor-RLuc expression, luminescence readings were also performed after 10 min of adding coelenterazine H. The net BRET was defined as [(530 nm emission)/(485 nm emission)]-cf.], where cf. corresponds to [(530 nm emission)/(485 nm emission)] for the receptor–RLuc expressed alone in the same experiment. BRET is expressed as milliBRET units (net BRETx1000). Data were fitted to a nonlinear regression equation with GraphPad Prism 6 software (GraphPad Software, San Diego, CA).

For bimolecular luminescent complementation (BiLC) assays, cells were co-transfected with the cDNA encoding for the receptors of interest fused to RLuc hemiproteins. After 48 h, cells were treated or not with the indicated TAT-TM peptides (4 μM) for 4 h at 37 °C. The quantification of the receptor-reconstituted RLuc expression was measured at 485 nm after 10 min of adding coelenterazine H. Cells expressing the receptor fused to one hemiprotein showed similar luminescence levels to non-transfected cells.

### 2.5. CODA-RET and receptor-G protein BRET assays

For complemented donor-acceptor resonance energy transfer (CODA-RET) assays, HEK-293T cells were co-transfected with human $G\alpha_{i1}$-mVenus or $G\alpha_{o1}$-mVenus (5 μg), untagged $G\beta_1$ (4.5 μg) and $G\gamma_2$ (5 μg) and the pair of receptors of interest fused to the corresponding RLuc hemiprotein (1.2 μg of $D_4R$-nRluc and 0.3 μg of $\alpha_{2A}R$-cRuc or 0.83 μg of $\alpha_{2A}R$-nRluc and 1.66 μg of $\alpha_{2A}R$-cRuc ). For receptor-G protein BRET assays, cells were co-transfected with human $D_{4.4}R$ or $D_{4.7}R$ (2 μg) fused to RLuc or with $\alpha_{2A}R$ fused (0.5 μg) to RLuc and unfused $D_{4.4}R$ or $D_{4.7}R$ (1 μg), as well as

with $G\alpha_{i1}$-mVenus or $G\alpha_{o1}$-mVenus (5 μg) and untagged $G\beta_1$ (4.5 μg) and $G\gamma_2$ (5 μg). The transfections were performed using polyethylenimine in a 1:2 ratio in 100-$cm^2$ cell culture plates. All experiments were performed approximately 48-hours after transfection. Cells were harvested, washed and resuspended in phosphate-buffered saline. Approximately 200,000 cells/well were distributed in 96-well plates, and 5 μM coelenterazine H was added to each well. 2.5 minutes after addition of coelenterazine H, agonists were added to each well. Antagonists were added 10 minutes before coelenterazine H. The fluorescence of the acceptor was quantified (excitation at 500 nm and emission at 540 nm for 1-second recordings) in a Mithras LB940 to confirm the constant expression levels across experiments. In parallel, the BRET signal from the same batch of cells was determined as the ratio of the light emitted by mVenus (530 nm) over that emitted by RLuc (485 nm). G protein-activation was calculated as the BRET change (BRET ratio for the corresponding drug minus BRET ratio in the absence of the drug) observed 10 minutes after the addition of ligands. $E_{max}$ values were expressed in absolute values or as the percentage of the effect of each ligand over the effect of NE or DA, depending on the experiment. Data were fitted to a nonlinear regression equation, assuming a single-phase dose-response curve with GraphPad Prism 6 software. The transfected amount and ratio among the receptor and heterotrimeric G proteins were tested for optimized dynamic range in drug-induced BRET. All ligands were purchased from either Sigma or Tocris.

### 2.6. Radioligand binding experiments

Radioligand binding experiments were performed in HEK-293T cells co-expressing the $\alpha_{2A}$-RLuc and the $D_4R$ and in brains of male and female sheep of 4-6 months old freshly obtained from the local slaughterhouse. Brain tissues and cell suspensions, were disrupted with a Polytron homogenizer (PTA 7 rotor, setting 3; Kinematica, Basel, Switzerland) for two 5 s-periods in 10 volumes of 50 mM Tris-HCl buffer, pH 7.4, containing a protease inhibitor cocktail (Sigma). Membranes were obtained by centrifugation twice at 105.000 g for 45 min at 4°C. The pellet was stored at −80°C, washed once more as described above and resuspended in 50 mM Tris-HCl buffer for immediate use. Membrane protein was quantified by the bicinchoninic acid method (Pierce Chemical Co., Rockford, IL, USA) using bovine serum albumin dilutions as standard.

Binding experiments were performed with membrane suspensions (0.2 mg of protein/mL) at room temperature in 50 mM Tris-HCl buffer, pH 7.4, containing 10 mM $MgCl_2$. For $\alpha_2R$ saturation-binding assays, membrane suspensions of HEK-293T cells co-expressing the $\alpha_{2A}$-RLuc and $D_{4.4}R$ were incubated for 3 h with increasing concentrations of the $\alpha_2R$ antagonist [$^3$H]RX821002 (PerkinElmer, Boston, MA, USA). Non-specific binding was determined in the presence of 10 μM of the non-radiolabeled antagonist RX821002 (Tocris, Bristol, United Kingdom). For $D_4R$ saturation-binding assays, membrane suspensions of the same cells were incubated for 3 h with increasing concentrations of [$^3$H]YM-09151-2 (PerkinElmer). Nonspecific binding was determined in the presence of 30 μM of dopamine (Sigma), because at this concentration dopamine does not displace the radioligand from sigma receptors.

For competition-binding assays, membrane suspensions were incubated for 2 h with a constant free concentration of 0.9 nM of the $\alpha_2$R antagonist [$^3$H], or 0.7 nM of the $D_2$-like receptor antagonist [$^3$H]YM-09151-2 and free increasing concentrations of each tested ligand.

In dissociation kinetic assays, membranes were pre-incubated at 12°C in 50 mM Tris HCl buffer, pH 7.4, containing 10 mM $MgCl_2$ in the absence or presence of A-412997 (30 nM). After 30 min, 0.9 nM of the $\alpha_2$R antagonist [$^3$H]RX821002 was added for an additional 1-h period of radioligand association. Dissociation was initiated by the addition of 10 μM of RX821002. At the indicated time intervals, total binding was measured as described below.

In all cases, free and membrane-bound ligands were separated by rapid filtration of 500 μL aliquots in a cell harvester (Brandel, Gaithersburg, MD, USA) through Whatman GF/C filters embedded in 0.3% polyethylenimine that were subsequently washed for 5 s with 5 mL of ice-cold 50 mM Tris-HCl buffer. The filters were incubated with 10 mL of Ultima Gold MV scintillation cocktail (PerkinElmer, Waltham, Massachusetts, USA) overnight at room temperature and radioactivity counts were determined using a Tri-Carb 2800 scintillation counter (PerkinElmer) with an efficiency of 62% [32].

### 2.7. Binding data analysis

Data were analyzed according to the 'dimer receptor model' of Casadó *et al.* (2007). The model assumes GPCR dimers as a main functional unit and provides a more robust analysis of parameters obtained from saturation and competition experiments with orthosteric ligands, as compared with the commonly used 'two-independent-site model' [33,34]. In competition experiments, the model analyzes the interactions of the radioligand with a competing ligand and it provides the affinity of the competing ligand for the first protomer in the unoccupied dimer ($K_{DB1}$), the affinity of the competing ligand for the second protomer when the first protomer is already occupied by the competing ligand ($K_{DB2}$) or the radioligand ($K_{DAB}$), and an index of cooperativity of the competing ligand ($D_{CB}$). A positive or negative value of $D_{CB}$ implies either an increase or a decrease in affinity of $K_{DB2}$ versus $K_{DB1}$ and its absolute value provides a measure of the degree of increase or decrease in affinity.

Radioligand curves were analyzed by nonlinear regression using the commercial Grafit curve-fitting software (Erithacus Software, Surrey, UK), by fitting the binding data to the mechanistic dimer receptor model, as described in detail elsewhere [35].

Saturation assays data must be fitted to Eq. (1).

$$A_{bound} = \frac{\left(K_{DA2}\, A + 2A^2\right) R_T}{\left(K_{DA1}K_{DA2} + K_{DA2}\, A + A^2\right)} \quad \text{Eq. (1)}$$

where $A$ represents the free radioligand concentration, $R_T$ is the total amount of receptor dimers, and $K_{DA1}$ and $K_{DA2}$ are the macroscopic equilibrium dissociation constants describing the binding of the first and the second ligand molecule to the receptor

homodimer. Nevertheless, in non-cooperative conditions, $K_{DA2}/K_{DA1} = 4$. Then, $K_{DA1}$ is enough to characterize the binding. Therefore, Eq. (1) can be reduced to Eq. (2):

$$A_{bound} = \frac{2\ A\ R_T}{2K_{DA1} + A} \quad \text{Eq. (2)}$$

To calculate the macroscopic equilibrium dissociation constants from competition experiments, the following general equation (Eq. (3)) must be applied:

$$A_{bound} = \frac{\left(K_{DA2}A + 2A^2 + \frac{K_{DA2}A\ B}{K_{DAB}}\right) R_T}{K_{DA1}K_{DA2} + K_{DA2}A + A^2 + \frac{K_{DA2}A\ B}{K_{DAB}} + \frac{K_{DA1}K_{DA2}B}{K_{DB1}} + \frac{K_{DA1}K_{DA2}B^2}{K_{DB1}K_{DB2}}} \quad \text{Eq. (3)}$$

where B represents the assayed competing compound concentration. However, in absence of cooperativity of the radioligand and non-allosteric modulation between A and B, Eq. (3) can be simplified due to the fact that: $K_{DA2} = 4K_{DA1}$ and $K_{DAB} = 2K_{DB1}$ (Eq. (4)):

$$A_{bound} = \frac{\left(4K_{DA1}A + 2A^2 + \frac{2K_{DA1}A\ B}{K_{DB1}}\right) R_T}{4K_{DA1}{}^2 + 4K_{DA1}A + A^2 + \frac{2K_{DA1}A\ B}{K_{DB1}} + \frac{4K_{DA1}{}^2B}{K_{DB1}} + \frac{4K_{DA1}{}^2B^2}{K_{DB1}K_{DB2}}} \quad \text{Eq. (4)}$$

For an absence of cooperativity and allosteric modulation between A and B, Eq. (3) can be simplified due to the fact that: $K_{DA2} = 4K_{DA1}$, $K_{DB2} = 4K_{DB1}$ and $K_{DAB} = 2K_{DB1}$ (Eq. (5)):

$$A_{bound} = \frac{\left(4K_{DA1}A + 2A^2 + \frac{2K_{DA1}A\ B}{K_{DB1}}\right) R_T}{4K_{DA1}{}^2 + 4K_{DA1}A + A^2 + \frac{2K_{DA1}A\ B}{K_{DB1}} + \frac{4K_{DA1}{}^2B}{K_{DB1}} + \frac{K_{DA1}{}^2B^2}{K_{DB1}{}^2}} \quad \text{Eq. (5)}$$

Dissociation kinetic data were fitted to the following empirical equation (Eq. (6)):

$$A_{total\ bound} = \sum_{i=1}^{n} A_{ei}e^{-tk_i} + A_{nonspecific\ bound} \quad \text{Eq. (6)}$$

where $A_{ei}$ represents the initial radioligand (the $\alpha_2$R antagonist [$^3$H]RX821002) bound at equilibrium for each molecular specie $i$, $t$ is time, and $k_i$ is the dissociation rate constants for the $n$ different molecular species. For biphasic curves (or complex dissociation kinetics), $n$ = 2.

### 2.8. cAMP production

For cAMP production, homogeneous time-resolved fluorescence energy transfer (HTRF) assays were performed using the Lance Ultra cAMP kit (PerkinElmer), based on competitive displacement of a europium chelate-labelled cAMP tracer bound to a specific antibody conjugated to acceptor beads. HEK-293T cells stably expressing $D_{4.4}R$ or $D_{4.7}R$ were transfected with $\alpha_{2A}$-RLuc receptor. First of all we established the optimal cell density and forskolin concentration for an appropriate fluorescent signal that covered most of the dynamic range of cAMP standard curve. Cells (1,200 cells/well) growing in medium containing 30 μM zardaverine were pretreated with the antagonists or the corresponding vehicle in white ProxiPlate 384-well microplates (PerkinElmer) at 25°C for 15 min and stimulated with agonists for 15 min before adding 0.5 μM forskolin (Sigma) or vehicle and incubating for an additional 15-min period. Fluorescence at 665 nm was analyzed on a PHERAstar Flagship microplate reader equipped with an HTRF optical module (BMG Lab technologies, Offenburg, Germany).

### 2.9. ERK1/2 phosphorylation assay

HEK-293T cells stably expressing $D_{4.4}R$ or $D_{4.7}R$ were transfected with $\alpha_{2A}$-RLuc receptor. The day of the experiment, cells were starved by treating them with serum free media for 4h at 37°C. After that, cells were incubated with the indicated agonist for 5 minutes at 37°C. Then, cells were rinsed with ice-cold phosphate-buffered saline and lysed by adding 200 ml ice-cold lysis buffer (50 mM Tris-HCl [pH 7.4], 50 mM NaF, 150 mM NaCl, 45 mM β-glycerophosphate, 1% Triton X-100, 20 mM phenylarsine oxide, 0.4 mM $NaVO_4$, and protease inhibitor cocktail). The cellular debris was removed by centrifugation at 13,000 x g for 5 minutes at 4°C, and the protein was quantified. To determine the level of ERK1/2 phosphorylation, equivalent amounts of protein were separated by electrophoresis on a denaturing 10% SDS-polyacrylamide gel and transferred onto polyvinylidene fluoride membranes. Odyssey blocking buffer (LI-COR Biosciences, Lincoln, NE) was then added, and the membrane was rocked for 90 minutes. The membranes were then probed with a mixture of a mouse anti– phospho-ERK1/2 antibody (1:2500; Merck, Darmstadt, Germany) and rabbit anti-ERK1/2 antibody that recognizes both phosphorylated and nonphosphorylated ERK1/2 (1:40,000; Merck) overnight at 4°C. The 42- and 44-kDa bands corresponding to ERK1 and ERK2 were visualized by the addition of a mixture of IRDye 800 (anti-mouse) antibody (1:10,000; Sigma) and IRDye 680 (anti-rabbit) antibody (1:10,000; Sigma) for 2 hours and scanned by the Odyssey infrared scanner (LICOR Biosciences). Band densities of western-blot images were quantified using the scanner software and exported to Excel (Microsoft, Redmond, WA). The level of phosphorylated ERK1/2 isoforms was normalized for differences in loading using the total ERK1/2 protein band intensities.

### 2.10. Animals and brain slices preparation

All animals used in the study were maintained in accordance with the guidelines of the National Institutes of Health (NIH) Animal Care, and the animal research conducted to perform this study was reviewed and approved by the NIDA IRP Animal Care and Use

Committee (protocol #15-BNRB-73). Procedures using rodents were also approved by the Ethical Committee for Animal Use of the University of Barcelona (OB 408/18 i OB 409/18).

Transgenic $D_{4.7}R$ mice, with a humanized mouse *DRD4* gene containing seven TRs of the human DRD4 in the homologous region of the mouse gene, which codes for the 3IL [5], were used. Homozygous $D_{4.7}R$ and WT littermates were obtained from a breeding colony of $D_{4.7}R$ heterozygous mice (in a C57Bl/6J background) kept in the National Institute on Drug Abuse, Intramural Research Program (NIDA IRP) breeding facility. Animals were housed (four per cage) and kept on a 12-hour light/12-hour dark cycle with food and water available *ad libitum*. Animals were killed by cervical dislocation. Mice brains were rapidly removed and placed in ice-cold oxygenated (95% $O_2$/5% $CO_2$) Krebs-$HCO_3^-$ buffer (containing [in mM]: 124 NaCl, 4 KCl, 1.25 $KH_2PO_4$, 1.5 $MgCl_2$, 1.5 $CaCl_2$, 10 glucose, and 26 $NaHCO_3$, pH 7.4). The brains were sliced coronally at 4°C. Slices containing cortex (500 μm thick) were kept at 4°C in this Krebs-$HCO_3$-buffer during the dissection and were transferred into an incubation tube containing 1 ml of ice-cold Krebs-$HCO_3$-buffer. The temperature was raised to 23°C, and after 30 min the medium was replaced by 2 ml of fresh Krebs-$HCO_3$-buffer (23°C). The slices were incubated under constant oxygenation ($O_2$/$CO_2$: 95%/5%) at 30°C for 4–5 h in absence or presence of the TM peptides at 4 μM in an Eppendorf Thermomixer (5 Prime, Boulder, Colorado, USA).

For phospho-ERK1/2 determination, the media was replaced by 200 μL of fresh Krebs-$HCO_3$-buffer and incubated for 30 min before the addition of any agent. Slices were treated or not with the indicated ligand for 5 min at 30°C. After the indicated incubation period, the solution was discarded, and slices were frozen on dry ice, lysed by the addition of 500 μL of ice-cold lysis buffer and treated as described for cells.

### 2.11. In situ PLAs in brain tissues and transfected cells

For proximity ligation assays (PLA) in brain tissues, mouse cortex slices (500 μm thick) were incubated or not with TM peptides at 4 μM as described above for phospho-ERK1/2 determination. Slices were then fixed by immersion in 4% paraformaldehyde solution for 1 h at 4°C. Samples were then washed in 50 mM Tris-HCl, 0.9% NaCl pH 7.8 buffer (TBS), cryopreserved in a 30% sucrose solution for 48 h at 4°C, and stored at −20°C until sectioning. 20 μm-thick slices were cut coronally on a freezing cryostat (Leica Jung CM-3000), mounted on slide glass and frozen at −20°C until use. To perform the PLA, slices were thawed at 4°C, washed in TBS, permeabilized with TBS containing 0.01% Triton X-100 for 10 min, and successively washed with TBS. For cell-based PLA, HEK-293T were grown on glass coverslips and transfected with 0.01 μg of cDNA corresponding to $_{2A}R$, $D_{4.4}R$ or $D_{4.7}R$, or co-transfected with both $_{2A}R$ and $D_4Rs$. 48 hours after transfection, cells were fixed in 4% paraformaldehyde for 15 min, washed with PBS containing 20 mM glycine, permeabilized with the same buffer containing 0.05% Triton X-100, and successively washed with PBS. In both cases, heteromers were detected using the Duolink in situ PLA detection Kit (Sigma) and following the instructions of the supplier. To detect $\alpha_{2A}R$-$D_4R$ heteromers, a mixture of equal amounts (1:100) of rabbit anti-$\alpha_{2A}R$ antibody (ab92650) (Thermo Scientific, Fremont, California, USA) and goat anti-$D_4R$ (sc-1439) (Santa Cruz Biotechnology, Santa Cruz, California, USA) antibody

were used. Samples were further incubated with anti-rabbit plus and anti-goat minus PLA probes (1:5). Slices were mounted using the mounting medium with DAPI and observed in a Leica SP2 confocal microscope (Leica Microsystems, Mannheim, Germany) equipped with an apochromatic 63X oil-immersion objective (N.A. 1.4), and a 405 nm and a 561 nm laser line. For each field of view, a stack of two channels (one per staining) and 9 to 15 Z stacks with a step size of 1 μm were acquired. Images were opened and processed using Image J (https://fiji.sc/). In tissue, a quantification of cells containing one or more red spots versus total cells (blue nuclei) was determined considering a total of 1,500–3,000 cells from 4–12 different fields (63X) within each region from three different animals. The ImageJ confocal program using the Fiji package was used. Nuclei and red spots were counted on the maximum projections of each image stack. After getting the projection, each channel was processed individually. The nuclei were segmented by filtering with a median filter, subtracting the background, enhancing the contrast with the contrast limited adaptive histogram equalization (CLAHE) plug-in, and finally applying a threshold to obtain the binary image and the regions of interest (ROIs) around each nucleus. Red spot images were also filtered and thresholded to obtain the binary images. Red spots were counted in each of the ROIs obtained in the nuclei images.

### 2.12. Statistical analysis

In binding assays, goodness of fit was tested according to reduced chi-squared value given by the regression program. The test of significance for two different model population variances was based upon the F-distribution using built-in functions in GraFit software. A probability greater than 95% ($p < 0.05$) was considered the criterion to select a more complex model (cooperativity) over the simplest one (non-cooperativity). Other statistical analyses were performed using GraphPad Prism 6 software. Differences between experimental group pairs were analyzed with unpaired two-sided Student's *t*-test. Differences among more than two groups of results were performed by one-way ANOVA (followed by Dunnett's or Bonferroni's *post hoc* test comparison). In all cases, data were presented as mean ± standard error of the mean (SEM). A level of $p < 0.05$ was considered as critical for assigning statistical significance.

## 3. Results

### 3.1. $D_{4.4}R$ and $D_{4.7}R$ form heteromers with $\alpha_{2A}R$ in mammalian transfected cells

First, we analyzed the ability of human $D_{4.4}R$ and $D_{4.7}R$ to form heteromers with human $\alpha_{2A}R$ in vitro by using BRET saturation assays. These experiments were performed in HEK-293T cells co-transfected with $\alpha_{2A}R$ cDNA fused to *Renilla* Luciferase ($\alpha_{2A}R$-RLuc) and increasing amounts of $D_{4.4}R$ or $D_{4.7}R$ cDNAs fused to yellow fluorescent protein ($D_{4.4}R$-YFP or $D_{4.7}R$-YFP, respectively). In both cases, BRET saturation curves were hyperbolic, indicating a specific interaction between both fusion proteins (Fig. 1A, B). $BRET_{max}$ values for $\alpha_{2A}R$-$D_{4.4}R$ were 98±7 milli BRET units (mBU) (n=8) and significantly lower values, 33±2 mBU (n=8), were obtained for $\alpha_{2A}R$-$D_{4.7}R$, (non-paired Student's *t* test: $t(14)= 8.928$, $p < 0.001$). This could indicate a reduced ability of $D_{4.7}R$ to heteromerize with $\alpha_{2A}R$, as compared with $D_{4.4}R$, although, most probably it reflects reduced BRET between the intracellularly localized RLuc and YFP due to a hindrance effect

related to the large 3IL of $D_{4.7}R$. Nevertheless, $BRET_{50}$ values are more indicative of the avidity to heteromerize and were significantly lower (more avidity) for $\alpha_{2A}R$-$D_{4.4}R$ (14±2) than for $\alpha_{2A}R$-$D_{4.7}R$ (60±10) (non-paired Student's *t* test: t(14)= 4.511, $p < 0.01$). The specificity of the $D_4Rs$ and $\alpha_{2A}R$ to form heteromers was supported by the observation of a linear, non-saturable BRET signal when cells were co-transfected with $\alpha_{2A}R$-RLuc cDNA and increasing amounts of $\alpha_{1A}R$-YFP cDNA (fig. S1A) or adenosine $A_1$ receptor ($A_1R$)-RLuc cDNA and increasing amounts of $D_{4.4}R$-YFP cDNA (fig. S1B), indicative of non-specific random collision of the corresponding fused receptors.

### 3.2. The allosteric modulation of [$^3$H]RX821002 binding to $\alpha_{2A}R$ is dependent on the $D_4R$ isoform heteromerization

We then evaluated the specificity of different ligands for $\alpha_2Rs$, $D_{4.4}R$ and $D_{4.7}R$, due to the previously described promiscuity of ligands for Gi-coupled dopamine and noradrenergic receptors [3,36]. To this end, we performed binding saturation experiments with the $\alpha_2R$ antagonist [$^3$H]RX821002 in HEK-293T cells transiently transfected with the human $\alpha_{2A}R$ cDNA and obtained a $K_{DA1}$ value for [$^3$H]RX821002 of 0.62±0.05 nM (n=3) (fig. S2A). Using the same technique we determined that the affinity ($K_{DA1)}$ of the $D_2$-like receptor antagonist [$^3$H]YM-09151-2 in HEK-293T cells stably transfected with $D_{4.4}R$ HEK-293T was 0.06±0.01 nM (n=3) (fig. S2B). We then performed competitive inhibition experiments using [$^3$H]RX821002 and the putative selective $D_4R$ agonists PD168077 and A-412997 in membrane preparations from sheep cortex. PD168077 and A-412997 showed a $K_{DB1}$ for $\alpha_2R$ of 80±10 nM (n=3) and 1,400±200 nM (n=3), respectively (fig. S2C). These affinities were nevertheless much lower than the affinity of the $\alpha_2R$ agonist dexmedetomidine, which showed a $K_{DB1}$ value of 0.009±0.001 nM and a $K_{DB2}$ of 0.40±0.02 nM (n= 5) (fig. S2C). Competitive inhibition experiments with [$^3$H]YM-09151-2 versus dexmedetomidine and A-412997 in membrane preparations from HEK-293T cells co-expressing $\alpha_{2A}R$ and $D_{4.4}R$ showed $K_{DB1}$ values of about 2,000-6,000 nM (n=3) and 1.1±0.1 nM (n=3), respectively (fig. S2D), while RX821002 did not displace [$^3$H]YM-09151-2 at any concentration up to 10 μM, indicating that RX821002 does not bind to $D_4Rs$ (fig. S2D). Also, in HEK-293T cells co-expressing $\alpha_2R$ and $D_{4.4}R$, dexmedetomidine displaced [$^3$H]RX821002 with a $K_{DB1}$ of 5.6±0.8 nM (n=6) (fig. S2E). Therefore, to study the function of $\alpha_2R$-$D_4R$ heteromers, A-412997 and dexmedetomidine were chosen as selective $D_4Rs$ and $\alpha_2Rs$ agonists, respectively. The expression of $D_4R$ and $\alpha_{2A}R$ in HEK-293T cells stably transfected with either $D_{4.4}R$ or $D_{4.7}R$ and transiently co-transfected with $\alpha_{2A}R$ was about 0.5-1 and 0.3-0.4 pmol/mg protein, respectively.

One of the characteristics of GPCR heteromers is their ability to mediate allosteric modulations between orthosteric ligands of their molecularly different receptor units (protomers). A ligand of one of the protomers can modify the affinity or efficacy of a ligand for the other molecularly different protomer [34]. Experiments of radioligand dissociation can resolve this type of allosteric interactions at the level of ligand binding [37–39]. Significant changes in the dissociation kinetic parameters of an orthosteric ligand by another ligand that does not bind to the same orthosteric site indicate an allosteric modulation [37]. In a GPCR heteromer, the binding of one ligand to the orthosteric site of one protomer can allosterically alter the kinetic properties of the other ligand bound to molecularly

different protomer [38]. We first evaluated the possibility of $D_4R$ ligands to allosterically modulate the binding of [$^3$H]RX821002 in membrane preparations of HEK-293T cells stably expressing $D_{4.4}R$ or $D_{4.7}R$ and transiently expressing $\alpha_{2A}R$. In cells expressing $\alpha_{2A}R$ and $D_{4.4}R$, dissociation curves of the $\alpha_{2A}R$ radioligand were biphasic and the $D_4R$ agonist A-412997 significantly modified both the slow and the fast dissociation rate constants of [$^3$H]RX821002 (Fig. 1C, D, and Table 1), indicative of an allosteric modulation between the two orthosteric $\alpha_{2A}R$ and $D_{4.4}R$ ligands and, therefore, an additional demonstration of $\alpha_{2A}R$-$D_{4.4}R$ heteromerization. The higher dissociation rate constants in the presence of the $D_4R$ agonist A-412997 (lower residence time, RT) indicate a negative allosteric modulation by the $D_4R$ agonist binding to the $D_{4.4}R$ on $\alpha_{2A}R$ antagonist binding. On the other hand, the dissociation curves of [$^3$H]RX821002 in cells expressing $\alpha_{2A}R$ and $D_{4.7}R$ were monophasic and A-412997 was not able to modify the dissociation rate constant of the labeled $\alpha_{2A}R$ antagonist (Fig. 1C, D, and Table 1). These results indicate a functional difference between $\alpha_{2A}R$-$D_{4.4}R$ and $\alpha_{2A}R$-$D_{4.7}R$ heteromers, such that $D_4R$ agonists can allosterically modulate $\alpha_{2A}R$ antagonist binding in the $\alpha_{2A}R$-$D_{4.4}R$ but not in the $\alpha_{2A}R$-$D_{4.7}R$ heteromer.

### 3.3. Gi protein activation by $\alpha_{2A}R$-$D_4R$ heteromers depends on the $D_4R$ polymorphic variant involved

We next sought to study G protein activation by $\alpha_{2A}R$-$D_{4.4}R$ and $\alpha_{2A}R$-$D_{4.7}R$ heteromers using CODA-RET assays [40]. In these experiments, two complementary halves of RLuc8 (nRLuc and cRLuc) are separately fused to two receptor molecules putatively able to oligomerize and the mVenus variant of YFP fused the α-helical domain of the $G\alpha_{i1}$ subunit. Ligand-induced changes in CODA-RET measurements imply, first, a successful complementation of RLuc, confirming the oligomerization of the corresponding protomers and, second, it represents the reading of a specific ligand-induced G protein activation through the GPCR oligomer [40,41]. Using CODA-RET, we determined the potency and efficacy of several adrenergic and dopaminergic ligands (DA and NE, the $D_2$-like receptor agonists pramipexole, ropinirole and rotigotine, the selective $D_4R$ agonist A-412997 and the $\alpha_2R$ agonists dexmedetomidine, clonidine and guanfacine) at activating $G\alpha_{i1}$ protein coupled to either the $\alpha_{2A}R$-$\alpha_{2A}R$ homomer or the $\alpha_{2A}R$-$D_{4.4}R$ or $\alpha_{2A}R$-$D_{4.7}R$ heteromers.

HEK-293T cells were co-transfected with $\alpha_{2A}R$ fused to cRLuc, $\alpha_{2A}R$, $D_{4.4}R$ or $D_{4.7}R$ fused to nRLuc, $G\alpha_{i1}$ subunit fused to mVenus and untagged $G\beta_1$, and $G\gamma_2$ subunits (see schematic representation in Fig. 2J–L). The amount of $G\alpha_{i1}$ subunits (or $G\alpha_{o1}$ subunits, see below) transfected produced values between 15,000 and 30,000 fluorescence units and the amount of RLuc receptor complementation produced values between 1 and 3 million (arbitrary units). A concentration-response of the ligand-induced change in BRET values allowed determining the potency and the relative efficacy (*versus* NE) of ligand-induced G protein activation by the three oligomers: $\alpha_{2A}R$-$\alpha_{2A}R$ homomers, $\alpha_{2A}R$-$D_{4.4}R$ heteromers and $\alpha_{2A}R$-$D_{4.7}R$ heteromers. $EC_{50}$ and $E_{max}$ values were obtained by fitting the data to sigmoidal concentration-response curves (Fig. 2A–C, and Table 2). The results show a non-canonical activation of $\alpha_{2A}R$-$\alpha_{2A}R$ by DA, with lower potency (12 *versus* 6 μM) (non-paired Student's *t* test: t(19)= 3.298, $p < 0.01$) and efficacy (69%) (t(19)= 8.177, $p < 0.001$) than NE (Fig. 2A, and Table 2), as previously described in BRET experiments by analyzing

ligand-induced changes in the interaction between G protein subunits [36]. As expected, ropinirole, rotigotine and A-412997 were ineffective in the $\alpha_{2A}$R-$\alpha_{2A}$R homomer, but the $D_2$-like receptor agonist pramipexole activated $G\alpha_{i1}$ with similar potency and efficacy than DA (Fig. 2A, and Table 2). To our knowledge, this $\alpha_{2A}$R agonistic activity of pramipexole has not been previously reported. All three synthetic $\alpha_2$R agonists, dexmedetomidine, clonidine and guanfacine showed high potency (in the nanomolar range) but low efficacy (between 14 and 26% *versus* NE) for the $\alpha_{2A}$R-$\alpha_{2A}$R homomer (Fig. 2A, and Table 2).

The potency and efficacy of $G\alpha_{i1}$ activation by the endogenous neurotransmitters, NE and DA, acting on $\alpha_{2A}$R-$D_{4.4}$R or $\alpha_{2A}$R-$D_{4.7}$R heteromers looked similar to that of the $\alpha_{2A}$R-$\alpha_{2A}$R homomer. The three oligomers showed lower efficacy for DA as compared to NE (about 60-70%). The only significant and striking difference was a five-fold increase in NE potency on the $\alpha_{2A}$R-$D_{4.7}$R as compared with the $\alpha_{2A}$R-$D_{4.4}$R (Fig. 2B, C, and Table 2). To analyze the contribution of each receptor to the Gi protein activation by NE and DA within each oligomer, cells were pretreated with the $\alpha_2$R antagonist BRL44408 or the selective $D_4$R antagonist L745,870. BRL44408 significantly decreased the potency of NE and DA in the $\alpha_{2A}$R-$\alpha_{2A}$R homomer and in both $\alpha_{2A}$R-$D_4$R heteromers (Fig. 2D–I, and Table 3). Similar results were obtained with the $\alpha_{2A}$R antagonist yohimbine (fig. S3). In contrast, L745,870 only decreased significantly the effect of DA and NE in the $\alpha_{2A}$R-$D_{4.4}$R heteromer (Fig. 2E, H). The lack of antagonistic effects by L745,870 in the $\alpha_{2A}$R-$D_{4.7}$R heteromer suggests an inability of $D_{4.7}$R to activate Gi upon heteromerization with $\alpha_{2A}$R (Fig. 2F, I).

To discard a possible artifact related to a loss of function of $D_{4.7}$R due to its fusion to RLuc hemiproteins, we also evaluated the ability of DA and NE to promote Gi protein activation by binding to $D_{4.7}$R-$D_{4.7}$R and also $D_{4.4}$R-$D_{4.4}$R homomers (Fig. 3). DA and NE activated with a potency of 0.29±0.07 μM and 230±70 μM the $D_{4.4}$R-$D_{4.4}$R homodimer (Fig. 3A) and of 0.13±0.03 μM and 40±20 μM the $D_{4.7}$R-$D_{4.7}$R homodimer (Fig. 3B), respectively. The potency of NE to activate $\alpha_{2A}$R-$D_{4.4}$R heteromers (10±3 μM; Table 2) was similar to that observed for $\alpha_{2A}$R-$\alpha_{2A}$R homodimers (6±1 μM; Table 2), but significantly different to that found to activate $D_{4.4}$R-$D_{4.4}$R homodimers (230±70 μM) (one-way ANOVA followed by Tuckey's multiple comparison test, $p < 0.001$). Thus, these results indicate that $\alpha_{2A}$R is mostly responsible for NE-induced Gi activation of $\alpha_{2A}$R-$D_{4.4}$R heteromers. Overall, this suggests that the L745,870-induced decrease in the potency of NE for $\alpha_{2A}$R-$D_{4.4}$R heteromers is not due to a counteraction of the contribution of $D_{4.4}$R to Gi signaling, but to cross-antagonism. This is an allosteric mechanism commonly observed in GPCR heteromers, by which an antagonist binding to one protomer can modify the properties of an agonist binding to the other molecularly different protomer in the heteromer [42,43]. However, this allosteric modulation was not observed in the $\alpha_{2A}$R-$D_{4.7}$R heteromer, providing an additional pharmacological difference between the two polymorphic variants that depends on the heteromerization with $\alpha_{2A}$R. In the $\alpha_{2A}$R-$D_{4.4}$R heteromer, DA-induced Gi protein activation is most likely mediated by both $\alpha_{2A}$R and $D_{4.4}$R, since the potency of DA for the heteromer (7±2 μM; Table 2) represents an intermediate value between the potency for the $\alpha_{2A}$R-$\alpha_{2A}$R homodimer (12±1 μM; Table 2) and for the $D_{4.4}$R-$D_{4.4}$R homodimer (0.29±0.07 μM). Thus, in the $\alpha_{2A}$R-$D_{4.4}$R heteromer the decrease

in DA efficacy in the presence of L745,870 or BRL44408 is mostly due to their respective competitive antagonism for $D_{4.4}R$ and $\alpha_{2A}R$.

The lack of participation of $D_{4.7}R$ in Gi-mediated signaling in $\alpha_{2A}R$-$D_{4.7}R$ heteromers is also apparent when comparing the similar results obtained with synthetic ligands on $\alpha_{2A}R$-$D_{4.7}R$ heteromers and $\alpha_{2A}R$-$\alpha_{2A}R$ homomers. Nevertheless, these compounds behaved differently on $\alpha_{2A}R$-$D_{4.4}R$ heteromers (Fig. 2, Table 2). This type of difference agrees with the recently reported distinct ligand-induced Gi protein activation of the $D_{2S}R$-$D_{2S}R$ homomer and the $D_{2S}R$-$D_{4.4}R$ and $D_{2S}R$-$D_{4.7}R$ heteromers [1]. In those experiments, the profile of Gi activation by pramipexole and ropinirole with the $D_{2S}R$-$D_{2S}R$ homomer was different from that observed with the $D_{2S}R$-$D_{4.4}R$ heteromer, but indistinguishable from the profile of the $D_{2S}R$-$D_{4.7}R$ heteromer [1]. In the present experiments, pramipexole showed a significantly higher potency for the $\alpha_{2A}R$-$D_{4.4}R$ heteromer as compared with the $\alpha_{2A}R$-$\alpha_{2A}R$ homomer and $\alpha_{2A}R$-$D_{4.7}R$ heteromer, albeit with lower efficacy (Fig. 2A–C, and Table 2). Ropinirole and rotigotine produced a small $G\alpha_{i1}$ protein activation in $\alpha_{2A}R$-$D_{4.4}R$ transfected cells, while they did not produce any response within the $\alpha_{2A}R$-$\alpha_{2A}R$ homomer nor the $\alpha_{2A}R$-$D_{4.7}R$ heteromer (Fig. 2A–C, and Table 2). On the other hand, the three $\alpha_2R$ agonists, dexmedetomidine, clonidine and guanfacine showed a complete lack of efficacy for the $\alpha_{2A}R$-$D_{4.4}R$ heteromer, while for the $\alpha_{2A}R$-$D_{4.7}R$ heteromer they showed the same response as for the $\alpha_{2A}R$-$\alpha_{2A}R$ homomer (Fig. 2A–C, and Table 2). The selective $D_4R$ agonist A-412997 also failed to activate $G\alpha_{i1}$ protein by $\alpha_{2A}R$-$D_{4.4}R$ (Fig. 2B, and Table 2). Altogether, the results using the synthetic compounds confirmed that the heteromerization of $\alpha_{2A}R$ with $D_{4.7}R$, but not with $D_{4.4}R$, blunts the ability of dopaminergic ligands to promote $D_4R$-mediated Gi protein activation. On the other hand, heteromerization with $D_{4.4}R$, but not with $D_{4.7}R$, seems to blunt the ability of exogenous, but not endogenous, adrenergic ligands to promote $\alpha_{2A}R$-mediated Gi protein activation.

The lack of efficacy of the potent and selective $D_4R$ agonist A-412997 not only on $\alpha_{2A}R$-$D_{4.7}R$ but also on the $\alpha_{2A}R$-$D_{4.4}R$ heteromer did not fit with our initial interpretation of selective blunting of $D_4R$-mediated Gi protein activation in the $\alpha_{2A}R$-$D_{4.7}R$. Therefore, we also tested its ability to promote activation of Gi protein with $D_{4.4}R$-$D_{4.4}R$ and $D_{4.7}R$-$D_{4.7}R$ homomers in CODA-RET experiments. In fact, A-412997 behaved as a competitive antagonist of DA in both homomers, producing a pronounced shift to the right of the concentration-response curve of DA-mediated Gi protein within $D_{4.4}R$-$D_{4.4}R$ and $D_{4.7}R$-$D_{4.7}R$ homomers (Fig. 3).

### 3.4. Go protein activation by $\alpha_{2A}R$-$D_4R$ heteromers depends on the $D_4R$ polymorphic variant involved

The inability of A-412997 to promote Gi activation by any $D_4R$ homomer and heteromer is at odds with its previously described full agonist profile in mammalian transfected cells and in laboratory animals [44–46]. Since recent findings indicate that some ligands show functional selectivity for different inhibitory Gα subunits [36], we sought to compare the ability of A-412997 to activate $G\alpha_{i1}$ *versus* $G\alpha_{o1}$ subunits, by analyzing BRET changes in cells transfected with $D_{4.4}R$ or $D_{4.7}R$ fused to RLuc and $G\alpha_{i1}$ or $G\alpha_{o1}$ fused to YFP (Fig. 4A–C). As in $D_{4.4}R$-$D_{4.4}R$ and $D_{4.7}R$-$D_{4.7}R$ homomers (Fig. 3), A-412997 did not promote

$D_{4.4}R$- or $D_{4.7}R$-mediated $G\alpha_{i1}$ activation, but it did promote significant $G\alpha_{o1}$ activation with both $D_4R$ variants (Fig. 4A, B). In CODA-RET experiments (Fig. 4D–F), A-412997 promoted $G\alpha_{o1}$ activation by $\alpha_{2A}R$-$D_{4.4}R$ heteromer but not by the $\alpha_{2A}R$-$D_{4.7}R$ heteromer, in agreement with the selective blunting of signaling of $D_{4.7}R$ by endogenous or exogenous ligands when it heteromerizes with $\alpha_{2A}R$ seen in Fig. 2.

Although dexmedetomidine, clonidine and guanfacine are known $\alpha_{2A}R$ agonists [47,48], they failed to activate $G\alpha_{i1}$ in the $\alpha_{2A}R$-$D_{4.4}R$ heteromer and showed only a weak intrinsic efficacy on the $\alpha_{2A}R$-$\alpha_{2A}R$ homomer and the $\alpha_{2A}R$-$D_{4.7}R$ heteromer (Fig. 2A–C). Therefore, we evaluated the ability of dexmedetomidine to activate $\alpha_2R$ coupled to $G\alpha_{o1}$ with BRET experiments in cells transfected with $\alpha_{2A}R$ fused to RLuc and $G\alpha_{o1}$ fused to YFP and co-transfected with either $D_{4.4}R$ or $D_{4.7}R$ (Fig. 4G–I). We found that dexmedetomidine promotes a significant $\alpha_{2A}R$-mediated $G\alpha_{o1}$ activation in the presence of either $D_{4.4}R$ or $D_{4.7}R$ (Fig. 4G, H). A-412997 produced a significant 2- to 3-fold decrease in the potency of dexmedetomidine in the cells co-transfected with $D_{4.4}R$ but not with $D_{4.7}R$ (Fig. 4G, H). This decrease is indicative of a selective negative allosteric crosstalk between the two agonists in $\alpha_{2A}R$-$D_{4.4}R$ heteromers coupled to $G\alpha_{o1}$. Finally, CODA-RET experiments showed that dexmedetomidine was also able to activate $G\alpha_{o1}$ in both the $\alpha_{2A}R$-$D_{4.4}R$ and $\alpha_{2A}R$-$D_{4.7}R$ heteromers (Fig. 4D, E).

### 3.5. $D_4R$ modulation of $\alpha_{2A}R$-mediated signaling in mammalian transfected cells depends on the $D_4R$ isoform heteromerization

Since the BRET experiments demonstrated the functional and pharmacological differences between $\alpha_{2A}R$-$D_{4.4}R$ and $\alpha_{2A}R$-$D_{4.7}R$ heteromers and their distinct coupling to $G\alpha_{i1}$ or $G\alpha_{o1}$ subunits, we decided to identify possible differences in the signaling of $\alpha_{2A}R$-$D_{4.4}R$ and $\alpha_{2A}R$-$D_{4.7}R$ heteromers in a mammalian cell line without transfection of exogenous $G\alpha$ proteins. It is well known that most $G\alpha$ subunits are ubiquitous and each cellular subtype can express at least four or five $G\alpha$ subtypes in different proportions [49]. First, we studied adenylyl cyclase signaling, measuring the ability of the $\alpha_{2A}R$ and $D_4R$ agonists, alone or in combination, to counteract forskolin-induced cAMP accumulation in HEK-293T cells stably transfected with either $D_{4.4}R$ or $D_{4.7}R$ and transiently co-transfected with $\alpha_{2A}R$ ($\alpha_{2A}R$-$D_{4.4}R$ and $\alpha_{2A}R$-$D_{4.7}R$ cells) (Fig. 5A). Although both agonists inhibited cAMP accumulation, A-412997 was more effective than dexmedetomidine in $\alpha_{2A}R$-$D_{4.4}R$ cells. Since A-412997 showed to be ineffective at activating $\alpha_{2A}R$-$D_{4.7}R$ heteromers (either by coupling with $G\alpha_{i1}$ or $G\alpha_{o1}$ proteins) (Fig. 2C and 4E), its efficacy in $\alpha_{2A}R$-$D_{4.7}R$ cells most probably reflects the activation of $D_{4.7}R$ not forming heteromers with $\alpha_{2A}R$. As mentioned above, the transfected stable cell lines had an excess of $D_4R$ *versus* $\alpha_{2A}R$. In addition, in the $\alpha_{2A}R$-$D_{4.7}R$ cells, the effect of dexmedetomidine plus A-412997 was additive and significantly different from dexmedetomidine alone (Fig. 5A). On the other hand, the results obtained in $\alpha_{2A}R$-$D_{4.4}R$ cells were not additive and the combined treatment did not produce a significantly different effect compared with dexmedetomidine alone, indicating a negative crosstalk (Fig. 5A).

Similar to cAMP levels, both agonists induced significant ERK1/2 phosphorylation, which was additive in $\alpha_{2A}R$-$D_{4.7}R$ but not in $\alpha_{2A}R$-$D_{4.4}R$ cells, where the coactivation with both

agonists was not significantly different from A-412997 alone (Fig. 5B and fig. S4). Again, relative to the effect of dexmedetomidine, A-412997 was more effective in $\alpha_{2A}$R-$D_{4.4}$R cells than in $\alpha_{2A}$R-$D_{4.7}$R cells. Altogether, these experiments reproduced the results obtained with dexmedetomidine and A-412997 on $\alpha_{2A}$R-$D_{4.4}$R and $\alpha_{2A}$R-$D_{4.7}$R heteromer-mediated Go protein activation, with a specific inefficacy (or lower efficacy) of A-412997 in the $\alpha_{2A}$R-$D_{4.7}$R and a negative crosstalk in the $\alpha_{2A}$R-$D_{4.4}$R heteromer, but not in $\alpha_{2A}$R-$D_{4.7}$R.

### 3.6. $\alpha_{2A}$R-$D_4$R heteromers are expressed in the cerebral cortex of wild type and h$D_{4.7}$R knock-in mice

To determine whether $\alpha_{2A}$R and $D_4$R could form heteromers in native brain tissue, we used the PLA technique, designed to detect *in situ* two different proteins only when located in close proximity [50] (schematic representation appears in Fig. 6J). Using specific anti-$D_4$R and anti-$\alpha_{2A}$R antibodies, we analyzed the expression of putative $\alpha_{2A}$R-$D_4$R complexes in the cortex of knock-in h$D_{4.7}$R mice, which express a $D_4$R with a humanized 3IL corresponding to the $D_{4.7}$R, and WT littermates, which express a shorter third intracellular loop, comparable to the human $D_{4.2}$R [5]. We observed a great number of cells containing red dots (% of positive cells in Fig. 6A–C), compatible with the presence of $\alpha_{2A}$R-$D_4$R complexes in the cortex of mice of both genotypes, as compared with the staining in the corpus callosum (taken as negative control brain area) (Fig. 6D). Similar % of positive cells than in corpus callosum were obtained in cortical slices in which one of the primary antibodies of the PLA was missing (Fig. 6E). The specificity of the method to detect $\alpha_{2A}$R and $D_4$R complexes was validated by immunocytochemistry, comparing the labeling in cells transfected with the corresponding receptors and controls (fig. S5).

The heteromer disrupting peptide technique was then applied to demonstrate that $\alpha_{2A}$R-$D_4$R complexes identified by PLA in the mouse brain cortex represent bona fide $\alpha_{2A}$R-$D_4$R heteromers. This technique has been successfully used to identify GPCR heteromers both in mammalian transfected cells and in native tissues (see, for instance [38,51]). In order to asses which TM domains are forming the interface between the two protomers, we fused synthetic peptides with the amino sequence of several TM domains of the $\alpha_{2A}$R and $D_4$R to the HIV-transactivator of transcription peptide (TAT-TM peptides). We tested the ability of TM4, TM5, TM6 and TM7 of $D_4$R and $\alpha_{2A}$R to disrupt BiLC of $\alpha_{2A}$R fused to cRLuc and $D_{4.4}$R or $D_{4.7}$R fused to nRLuc (see Fig. 7A). Only TM4 of both $D_4$R and $\alpha_{2A}$R were able to significantly decrease the levels of luminescence, indicating that these TMs form part of the heteromeric interface (Fig. 7B). Cells transfected with $\alpha_{1A}$R-nRLuc and $\alpha_{2A}$R-cRLuc or with $D_{4.4}$R-nRLuc and $A_1$R-cRLuc were used as negative controls (Fig. 7B). In PLA experiments, in complete correlation with the BiLC experiments, TM4 (but not TM5 or TM7) of $D_4$R also decreased the number of cells expressing $\alpha_{2A}$R-$D_4$R complexes detected in the cerebral cortex of WT mice (Fig. 6F–I), indicating that these complexes correspond to $\alpha_{2A}$R-$D_4$R heteromers.

We next sought to examine the functional significance of $\alpha_2$R-$D_4$R heteromers in the brain cortex. If a significant population of $\alpha_{2A}$R in the mouse cerebral cortex forms heteromers with $D_4$R and preferentially couple to $G\alpha_o$ proteins, we should be able to observe the same qualitative differences in the pharmacological profile of dexmedetomidine and A-412997 in

cortical tissue from knock-in $hD_{4.7}R$ mice *versus* WT mice as those we previously described in $\alpha_{2A}R$-$D_{4.7}R$ cells *versus* $\alpha_{2A}R$-$D_{4.4}R$ cells (Fig. 5B). Dexmedetomidine and A-412997 administered alone produced a similar degree of MAPK activation in cortical slices from WT mice, while A-412997's effect was significantly weaker than of dexmedetomidine in $hD_{4.7}R$ mice (Fig. 8A, B). In addition, in WT mice, we found a negative crosstalk between dexmedetomidine and A-412997 evidenced by a significantly lower MAPK activation than that observed when either drug was administered alone (Fig. 8A). This negative crosstalk could be attenuated with the application of TM4 of the $D_4R$, which selectively disrupts $\alpha_{2A}R$-$D_4R$ heteromerization, but not with TM6 of the $D_4R$ (Fig. 8C–E). Thus, in WT mice, in the presence of TM4, but not TM6, of the $D_4R$, the combined treatment of dexmedetomidine and A-412997 produced about the same level of MAPK activation than either drug when administered alone. The same level of MAPK activation induced by dexmedetomidine alone or combined with A-412997 was observed in $hD_{4.7}R$ mice (Fig. 8B). Therefore, in contrast with the results obtained in transfected cells (Fig. 5B), the combined effects of $\alpha_{2A}R$ and $D_4R$ agonists did not exceed that of the activation of $\alpha_{2A}R$ alone, even in the presence of $D_{4.7}R$. This difference could be explained by a ceiling effect occurring in brain tissue. Altogether, the evident negative crosstalk observed in $\alpha_{2A}R$-$D_4R$ heteromers and the $D_{4.7}R$-dependent decrease in the effect of A-412997 indicate the existence of a significant population of functional $\alpha_{2A}R$-$D_4R$ heteromers in the mouse cerebral cortex.

## 4. Discussion

The results presented in this study demonstrate the presence of functional $\alpha_{2A}R$-$D_4R$ heteromers in mouse cerebral cortex. In addition, we show a functional difference in the function of the two most frequent human *DRD4* gene polymorphisms, $D_{4.4}R$ and $D_{4.7}R$ [13–15]. Synthetic peptides with the amino acid sequence of TM domains of GPCRs have become a very useful tool for the demonstration of GPCR oligomers, the identification of their putative oligomeric (homomeric and heteromeric) interfaces and their demonstration in native tissues (for recent studies, see [52–55]). In the present study, the application of synthetic peptides in experiments with PLA and $\alpha_{2A}R$ and $D_4R$ agonist-induced MAPK activation, allowed to demonstrate that $\alpha_{2A}R$-$D_4R$ heteromers constitute a significant functional population of $\alpha_{2A}R$ and $D_4R$ in the mouse cerebral cortex. The functional differences described here might help to explain the association of human polymorphisms of $\alpha_{2A}R$ and $D_4R$ genes with impulsivity and vulnerability to ADHD [13,16–20,26].

We used BRET assays to study the in vitro effect of endogenous ligands, DA and NE, and several synthetic ligands on their ability to promote activation of $G\alpha_{i/o}$ proteins by $\alpha_{2A}R$-$\alpha_{2A}R$ homomers and $\alpha_{2A}R$-$D_4R$ heteromers. The drugs showed notable pharmacological differences that depended on the G protein subtype ($G\alpha_{i1}$ or $G\alpha_{o1}$) and on the polymorphic variant of the $D_4R$. Recent results obtained with such assays allowed to extend the concept of functional selectivity, which generally implies the selectivity of some ligands in promoting biased G protein-dependent or G protein-independent signaling [56], to a G protein subunit-dependent functional selectivity [36,57]. More commonly, instead of a complete functional selectivity, this phenomenon implies that different ligands demonstrate different potencies and efficacies at activating different $G\alpha$ protein subunits [36,57].

In the present study, we report a G protein-subtype dependent functional selectivity of a $D_4R$ ligand, A-412997, which behaved as a potent and efficacious agonist at activating $G\alpha_{o1}$, whilst it behaved as a competitive antagonist at activating $G\alpha_{i1}$ with both $D_{4.4}R$ and $D_{4.7}R$. From a physiological point of view, $G\alpha_o$ proteins seem to be predominant in the brain, which would agree with the previously reported efficacy of A-412997 in animals [44–46]. In addition, to our knowledge, here we report for the first time a G protein-dependent functional selectivity that is not only dependent on receptor heteromerization, but on the polymorphic variant of one of the GPCR protomers of the heteromer. The endogenous ligands, NE and DA, were able to activate $G\alpha_{i1}$ by binding to the $\alpha_{2A}R$ forming $\alpha_{2A}R$ homomers and $\alpha_{2A}R$-$D_4R$ heteromers, as demonstrated by the counteracting effect of an $\alpha_{2A}R$ antagonist. On the other hand, the exogenous ligands dexmedetomidine, guanfacine and clonidine were unable to activate $G\alpha_{i1}$ with the $\alpha_{2A}R$-$D_{4.4}R$ heteromer. Yet, dexmedetomidine was effective at activating $G\alpha_{o1}$ with both $\alpha_{2A}R$-$D_{4.4}R$ and $\alpha_{2A}R$-$D_{4.7}R$ heteromers.

Another remarkable pharmacological difference between $\alpha_{2A}R$-$D_{4.4}R$ and $\alpha_{2A}R$-$D_{4.7}R$ heteromers was the loss of efficacy of any $D_4R$ agonists to promote activation of any G protein within the $\alpha_{2A}R$-$D_{4.7}R$ heteromer. Hence, the $D_{4.7}R$ appears to be a silent partner when present in the $\alpha_{2A}R$-$D_{4.7}R$ heteromer. Nevertheless, $\alpha_{2A}R$-$D_{4.7}R$ heteromerization significantly increased the potency of NE, by five times, representing a gain of function of the $\alpha_{2A}R$. This is reminiscent of the pharmacological properties of the $D_2R$-$D_{4.7}R$ heteromer, which is also associated with an increase in the potency of DA and a gain of function of the $D_2R$ (increase in constitutive activity; see Introduction and Sánchez-Soto *et al.*, 2019). In contrast, $D_{4.4}R$ can be activated by NE and DA when present in the $\alpha_{2A}R$-$D_{4.4}R$ heteromer, regardless of the G protein subtype. In addition, it promotes a negative crosstalk between $\alpha_{2A}R$ and $D_{4.4}R$ agonists. Here, we showed the ability of A-412997 to selectively decrease signaling induced by dexmedetomidine in HEK-293T cells expressing $\alpha_{2A}R$ and $D_{4.4}R$, but not $\alpha_{2A}R$ and $D_{4.7}R$. Together with the significant A-412997-induced signaling in $\alpha_{2A}R$-$D_{4.4}R$ cells and its attenuation in $\alpha_{2A}R$-$D_{4.7}R$ cells, these results also indicated that $G\alpha_o$ rather than $G\alpha_i$ proteins are primarily involved.

The results obtained in cortical tissue from WT and $hD_{4.7}R$ knock-in mice recapitulated the phenomena observed in cultured cells. In addition, the selective counteraction of the negative crosstalk with the $\alpha_{2A}R$-$D_4R$ heteromer disruptive peptide, demonstrated the existence of a significant population of $\alpha_{2A}R$-$D_4R$ heteromers in mouse cerebral cortex. Moreover, it indicated that in native tissue the heteromer is likely coupled to $G\alpha_o$ proteins. This led to two obvious questions: first, what is the functional role of $\alpha_{2A}R$-$D_4R$ heteromers and the different functional role of $\alpha_{2A}R$-$D_{4.4}R$ and $\alpha_{2A}R$-$D_{4.7}R$ heteromers; and second, how these differences relate to the human $D_4R$ variants and their associations with impulsivity, ADHD and SUD and their respective pharmacological treatment. A recent large meta-analysis [20] indicated that $D_{4.7}R$ is an ADHD risk factor in European-Caucasian populations and is linked to a poor treatment efficacy of methylphenidate, while $D_{4.4}R$ is a significant protective factor in European-Caucasian and South American populations and is also associated to a positive response to methylphenidate.

Previous studies have shown similar potencies for NE and DA at activating $D_{4.4}R$ or $D_{4.7}R$ when coupled to $G\alpha_{o1}$, while higher potencies for NE than DA are found for $\alpha_{2A}R$ [3,36]. Hence, both $\alpha_{2A}R$ and $D_{4.4}R$ protomers can be activated by NE and DA, at least with the $\alpha_{2A}R$-$D_{4.4}R$ heteromer. Our heuristic hypothesis is that the $\alpha_{2A}R$-$D_{4.4}R$ heteromer represents a fine-tune device that senses different concentrations of NE. Low NE concentrations activate $\alpha_{2A}R$ and higher NE concentrations or the simultaneous presence of DA also activates the $D_{4.4}R$, which exerts a negative crosstalk promoting a negative feedback. This inverted u-shaped function might provide a buffer mechanism responsible for resilience to the development of ADHD and for a therapeutic response to methylphenidate in the presence of the $\alpha_{2A}R$-$D_{4.4}R$, which is not as effective when acting on $\alpha_{2A}R$-$D_{4.7}R$ heteromers.

In summary, we demonstrate that $\alpha_{2A}R$ can form oligomeric complexes with $D_{4.4}R$ and $D_{4.7}R$ in transfected cells, that these heteromers constitute a significant functional population of $\alpha_{2A}R$ and $D_4R$ in mouse cerebral cortex and that their pharmacological and functional profiles depend on the $D_4R$ polymorphic variant involved. Taken together, our data indicate that $\alpha_{2A}R$-$D_4R$ heteromers need to be considered as novel targets for the development of therapeutic agents for ADHD and other impulsivity-related neuropsychiatric disorders and that the therapeutic benefits and strategies of these drugs must consider the differential properties of the most common human $D_4R$ variants (such as $D_{4.4}R$ and $D_{4.7}R$) present in the $\alpha_{2A}R$-$D_4R$ heteromers.

## Supplementary Material

Refer to Web version on PubMed Central for supplementary material.

## Acknowledgements

The authors thank Manel Bosch, of the Unitat de Microscopia Optica Avançada, Fac. of Biology, University of Barcelona, for the ImageJ macro to analyze PLA results and Mercè Batlle Pons and Maria Rosell Rebulà for their technical help. $G\alpha_i$-like plasmids were generously shared by Céline Galés (INSERM). This work was supported by the Spanish Ministerio de Economía y Competitividad" and the European Regional Development Funds of the European Union [SAF2014-54840-R to VC and EIC, and SAF2017-87629-R to VC and EIC]; the "Centro de Investigación Biomédica en Red sobre Enfermedades Neurodegenerativas" [CB06/05/0064]; the "Generalitat de Catalunya" [2017-SGR-1497]; the "Fundació La Marató de TV3" [20140610 to EIC]; and intramural funds of the National Institute on Drug Abuse to SF.

## Data availability

All data needed to evaluate the conclusions in the paper are present in the paper or the Supplementary Materials.

## Abbreviations:

| | |
|---|---|
| **$\alpha_{2A}R$** | $\alpha_{2A}$ adrenoceptor |
| **ADHD** | attention deficit hyperactivity disorder |
| **BiLC** | bimolecular luminescence complementation |
| **BRET** | bioluminescence resonance energy transfer |

| | |
|---|---|
| **CODA-RET** | complemented donor-acceptor resonance energy transfer |
| **$D_2R$** | dopamine $D_2$ receptor |
| **$D_4R$** | dopamine $D_4$ receptor |
| **DA** | dopamine |
| **DMT** | dexmedetomidine |
| **FK** | forskolin |
| **NE** | norepinephrine |
| **mBU** | milli BRET units |
| **PLA** | proximity ligation assay |
| **RLuc** | *Renilla* Luciferase |
| **RT** | residence time |
| **TAT** | HIV-transactivator of transcription peptide |
| **TM** | transmembrane |
| **YFP** | yellow fluorescent protein |

## References


[1]. Sánchez-Soto M, Yano H, Cai N-S, Casadó-Anguera V, Moreno E, Casadó V, Ferré S, Revisiting the Functional Role of Dopamine D4 Receptor Gene Polymorphisms: Heteromerization-Dependent Gain of Function of the D4.7 Receptor Variant, Mol. Neurobiol. 56 (2019). doi:10.1007/s12035-018-1413-1.

[2]. Root DH, Hoffman AF, Good CH, Zhang S, Gigante E, Lupica CR, Morales M, Norepinephrine activates dopamine d4 receptors in the rat lateral habenula, J. Neurosci. 35 (2015) 3460–3469. doi:10.1523/JNEUROSCI.4525-13.2015. [PubMed: 25716845]

[3]. Sánchez-Soto M, Bonifazi A, Cai NS, Ellenberger MP, Newman AH, Ferre S, Yano H, Evidence for Noncanonical Neurotransmitter Activation: Norepinephrine as a Dopamine D2-Like Receptor Agonist, Mol. Pharmacol. 89 (2016) 457–466. doi:10.1124/mol.115.101808. [PubMed: 26843180]

[4]. Gonzalez S, Moreno-Delgado D, Moreno E, Pérez-Capote K, Franco R, Mallol J, Cortés A, Casadó V, Lluís C, Ortiz J, Ferré S, Canela E, McCormick PJ, Circadian-related heteromerization of adrenergic and dopamine $D_4$ receptors modulates melatonin synthesis and release in the pineal gland., PLoS Biol. 10 (2012) e1001347. doi:10.1371/journal.pbio.1001347. [PubMed: 22723743]

[5]. Gonzalez S, Rangel-Barajas C, Peper M, Lorenzo R, Moreno E, Ciruela F, Borycz B, Ortiz J, Lluís C, Franco R, McCormick P, Volkow N, Rubinstein M, Floran B, Ferré S, Dopamine D4 receptor, but not the ADHD-associated D4.7 variant, forms functional heteromers with the dopamine D2S receptor in the brain, Mol. Psychiatry. 17 (2012) 650–662. doi:10.1038/mp.2011.93. [PubMed: 21844870]

[6]. Bonaventura J, Quiroz C, Cai N-S, Rubinstein M, Tanda G, Ferré S, Key role of the dopamine D 4 receptor in the modulation of corticostriatal glutamatergic neurotransmission, Sci. Adv. 3 (2017) e1601631. doi:10.1126/sciadv.1601631. [PubMed: 28097219]

[7]. Kim J-SS, Bailey MJ, Weller JL, Sugden D, Rath MF, Møller M, Klein DC, Thyroid hormone and adrenergic signaling interact to control pineal expression of the dopamine receptor D4 gene

(Drd4), Mol. Cell. Endocrinol. 314 (2010) 128–135. doi:10.1016/j.mce.2009.05.013. [PubMed: 19482058]

[8]. Bustos DM, Bailey MJ, Sugden D, Carter DA, Rath MF, Møller M, Coon SL, Weller JL, Klein DC, Global daily dynamics of the pineal transcriptome, Cell Tissue Res. 344 (2011) 1–11. doi:10.1007/s00441-010-1094-1. [PubMed: 21302120]

[9]. Tarazi FI, Campbell A, Yeghiayan SK, Baldessarini RJ, Localization of dopamine receptor subtypes in corpus striatum and nucleus accumbens septi of rat brain: comparison of D1-, D2-, and D4-like receptors., Neuroscience. 83 (1998) 169–76. doi:10.1016/s0306-4522(97)00386-2. [PubMed: 9466407]

[10]. Svingos AL, Periasamy S, Pickel VM, Presynaptic dopamine D4 receptor localization in the rat nucleus accumbens shell, Synapse. 36 (2000) 222–232. doi:10.1002/(SICI)1098-2396(20000601)36:3<222::AID-SYN6>3.0.CO;2-H. [PubMed: 10819901]

[11]. Lauzon NM, Laviolette SR, Dopamine D4-receptor modulation of cortical neuronal network activity and emotional processing: Implications for neuropsychiatric disorders, Behav. Brain Res. 208 (2010) 12–22. doi:10.1016/j.bbr.2009.11.037. [PubMed: 19948192]

[12]. Zhong P, Liu W, Yan Z, Aberrant regulation of synchronous network activity by the attention-deficit/hyperactivity disorder-associated human dopamine D4 receptor variant D4.7 in the prefrontal cortex, J. Physiol. 594 (2016) 135–147. doi:10.1113/JP271317. [PubMed: 26541360]

[13]. LaHoste GJ, Swanson JM, Wigal SB, Glabe C, Wigal T, King N, Kennedy JL, Dopamine D4 receptor gene polymorphism is associated with attention deficit hyperactivity disorder., Mol. Psychiatry 1 (1996) 121–4. http://www.ncbi.nlm.nih.gov/pubmed/9118321 (accessed September 4, 2019). [PubMed: 9118321]

[14]. Chang F-M, Kidd JR, Livak KJ, Pakstis AJ, Kidd KK, The world-wide distribution of allele frequencies at the human dopamine D4 receptor locus, Hum. Genet. 98 (1996) 91–101. doi:10.1007/s004390050166. [PubMed: 8682515]

[15]. Wang E, Ding YC, Flodman P, Kidd JR, Kidd KK, Grady DL, Ryder OA, Spence MA, Swanson JM, Moyzis RK, The Genetic Architecture of Selection at the Human Dopamine Receptor D4 (DRD4) Gene Locus, Am. J. Hum. Genet. 74 (2004) 931–944. doi:10.1086/420854. [PubMed: 15077199]

[16]. Faraone SV, Perlis RH, Doyle AE, Smoller JW, Goralnick JJ, Holmgren MA, Sklar P, Molecular Genetics of Attention-Deficit/Hyperactivity Disorder, Biol. Psychiatry. 57 (2005) 1313–1323. doi:10.1016/j.biopsych.2004.11.024. [PubMed: 15950004]

[17]. Li D, Sham PC, Owen MJ, He L, Meta-analysis shows significant association between dopamine system genes and attention deficit hyperactivity disorder (ADHD), Hum. Mol. Genet. 15 (2006) 2276–2284. doi:10.1093/hmg/ddl152. [PubMed: 16774975]

[18]. Gizer IR, Ficks C, Waldman ID, Candidate gene studies of ADHD: a meta-analytic review, Hum. Genet. 126 (2009) 51–90. doi:10.1007/s00439-009-0694-x. [PubMed: 19506906]

[19]. Belcher AM, Volkow ND, Moeller FG, Ferré S, Personality traits and vulnerability or resilience to substance use disorders, Trends Cogn. Sci. 18 (2014) 211–217. doi:10.1016/j.tics.2014.01.010. [PubMed: 24612993]

[20]. Bonvicini C, Cortese S, Maj C, Baune BBT, Faraone SSVS, Scassellati C, DRD4 48 bp multiallelic variants as age-population-specific biomarkers in attention-deficit/hyperactivity disorder, Transl. Psychiatry 10 (2020). doi:10.1038/s41398-020-0755-4.

[21]. Congdon E, Lesch KP, Canli T, Analysis of DRD4 and DAT polymorphisms and behavioral inhibition in healthy adults: Implications for impulsivity, Am. J. Med. Genet. Part B Neuropsychiatr. Genet 147 (2008) 27–32. doi:10.1002/ajmg.b.30557.

[22]. Belcher A, Lejuez C, Moeller F, Volkow N, Ferré S, Choice impulsivity. A drug-modifiable personality trait, in: Pickard H, Ahmed S (Eds.), Routledge Handb. Philos. Sci. Addict, Routledge, New York, 2018: pp. 286–298.

[23]. Sweitzer MM, Halder I, Flory JD, Craig AE, Gianaros PJ, Ferrell RE, Manuck SB, Polymorphic variation in the dopamine D4 receptor predicts delay discounting as a function of childhood socioeconomic status: Evidence for differential susceptibility, Soc. Cogn. Affect. Neurosci 8 (2013) 499–508. doi:10.1093/scan/nss020. [PubMed: 22345368]

[24]. Roman T, Schmitz M, V Polanczyk G, Eizirik M, Rohde LA, Hutz MH, Is the alpha-2A adrenergic receptor gene (ADRA2A) associated with attention-deficit/hyperactivity disorder?, Am. J. Med. Genet. B. Neuropsychiatr. Genet 120B (2003) 116–20. doi:10.1002/ajmg.b.20018. [PubMed: 12815749]

[25]. Park L, Nigg JT, Waldman ID, Nummy KA, Huang-Pollock C, Rappley M, Friderici KH, Association and linkage of α−2A adrenergic receptor gene polymorphisms with childhood ADHD, Mol. Psychiatry. 10 (2005) 572–580. doi:10.1038/sj.mp.4001605. [PubMed: 15520832]

[26]. Cummins TDR, Jacoby O, Hawi Z, Nandam LS, V Byrne MA, Kim B-N, Wagner J, Chambers CD, Bellgrove MA, Alpha-2A adrenergic receptor gene variants are associated with increased intra-individual variability in response time, Mol. Psychiatry. 19 (2014) 1031–1036. doi:10.1038/mp.2013.140. [PubMed: 24166412]

[27]. Erdozain AM, Brocos-Mosquera I, Gabilondo AM, Meana JJ, Callado LF, Differential α 2A - and α 2C -adrenoceptor protein expression in presynaptic and postsynaptic density fractions of postmortem human prefrontal cortex, J. Psychopharmacol. 33 (2019) 244–249. doi:10.1177/0269881118798612. [PubMed: 30255728]

[28]. Wang M, Ramos BP, Paspalas CD, Shu Y, Simen A, Duque A, Vijayraghavan S, Brennan A, Dudley A, Nou E, Mazer JA, McCormick DA, Arnsten AFT, α2A-Adrenoceptors Strengthen Working Memory Networks by Inhibiting cAMP-HCN Channel Signaling in Prefrontal Cortex, Cell. 129 (2007) 397–410. doi:10.1016/j.cell.2007.03.015. [PubMed: 17448997]

[29]. Brennan AR, Arnsten AFT, Neuronal mechanisms underlying attention deficit hyperactivity disorder: The influence of arousal on prefrontal cortical function, in: Ann. N. Y. Acad. Sci, Blackwell Publishing Inc., 2008: pp. 236–245. doi:10.1196/annals.1417.007.

[30]. Ji X-H, Ji J-Z, Zhang H, Li B-M, Stimulation of α2-Adrenoceptors Suppresses Excitatory Synaptic Transmission in the Medial Prefrontal Cortex of Rat, Neuropsychopharmacology. 33 (2008) 2263–2271. doi:10.1038/sj.npp.1301603. [PubMed: 17957212]

[31]. He SQ, Zhang ZN, Guan JS, Liu HR, Zhao B, Wang HB, Li Q, Yang H, Luo J, Li ZY, Wang Q, Lu YJ, Bao L, Zhang X, Facilitation of μ-Opioid Receptor Activity by Preventing δ-Opioid Receptor-Mediated Codegradation, Neuron. 69 (2011) 120–131. doi:10.1016/j.neuron.2010.12.001. [PubMed: 21220103]

[32]. Casadó-Anguera V, Moreno E, Mallol J, Ferré S, Canela EI, Cortés A, Casadó V, Reinterpreting anomalous competitive binding experiments within G protein-coupled receptor homodimers using a dimer receptor model, Pharmacol. Res. 139 (2019) 337–347. doi:10.1016/j.phrs.2018.11.032. [PubMed: 30472462]

[33]. Casadó V, Cortés A, Ciruela F, Mallol J, Ferré S, Lluis C, Canela EI, Franco R, Old and new ways to calculate the affinity of agonists and antagonists interacting with G-protein-coupled monomeric and dimeric receptors: the receptor-dimer cooperativity index., Pharmacol. Ther. 116 (2007) 343–54. doi:10.1016/j.pharmthera.2007.05.010. [PubMed: 17935788]

[34]. Ferré S, Casadó V, Devi LA, Filizola M, Jockers R, Lohse MJ, Milligan G, Pin J-P, Guitart X, G protein-coupled receptor oligomerization revisited: functional and pharmacological perspectives., Pharmacol. Rev 66 (2014) 413–34. doi:10.1124/pr.113.008052. [PubMed: 24515647]

[35]. Casadó V, Ferrada C, Bonaventura J, Gracia E, Mallol J, Canela EI, Lluís C, Cortés A, Franco R, Useful pharmacological parameters for G-protein-coupled receptor homodimers obtained from competition experiments. Agonist-antagonist binding modulation., Biochem. Pharmacol. 78 (2009) 1456–63. doi:10.1016/j.bcp.2009.07.012. [PubMed: 19643089]

[36]. Sánchez-Soto M, Casadó-Anguera V, Yano H, Bender BJ, Cai N-S, Moreno E, Canela EI, Cortés A, Meiler J, Casadó V, Ferré S, α2A- and α2C-Adrenoceptors as Potential Targets for Dopamine and Dopamine Receptor Ligands, Mol. Neurobiol. 55 (2018) 8438–8454. doi:10.1007/s12035-018-1004-1. [PubMed: 29552726]

[37]. May LT, Leach K, Sexton PM, Christopoulos A, Allosteric Modulation of G Protein–Coupled Receptors, Annu. Rev. Pharmacol. Toxicol. 47 (2007) 1–51. doi:10.1146/annurev.pharmtox.47.120505.105159. [PubMed: 17009927]

[38]. Bonaventura J, Navarro G, Casadó-Anguera V, Azdad K, Rea W, Moreno E, Brugarolas M, Mallol J, Canela EI, Lluís C, Cortés A, Volkow ND, Schiffmann SN, Ferré S, Casadó V, Allosteric interactions between agonists and antagonists within the adenosine A 2A receptor-

dopamine D 2 receptor heterotetramer, Proc. Natl. Acad. Sci. 112 (2015) E3609–E3618. doi:10.1073/pnas.1507704112. [PubMed: 26100888]

[39]. Casadó-Anguera V, Bonaventura J, Moreno E, Navarro G, Cortés A, Ferré S, Casadó V, Evidence for the heterotetrameric structure of the adenosine A2A-dopamine D2 receptor complex., Biochem. Soc. Trans. 44 (2016) 595–600. doi:10.1042/BST20150276. [PubMed: 27068975]

[40]. Urizar E, Yano H, Kolster R, Galés C, Lambert N, Javitch JA, CODA-RET reveals functional selectivity as a result of GPCR heteromerization, Nat. Chem. Biol. 7 (2011) 624–630. doi:10.1038/nchembio.623. [PubMed: 21785426]

[41]. Guitart X, Navarro G, Moreno E, Yano H, Cai N-S, Sanchez-Soto M, Kumar-Barodia S, Naidu YT, Mallol J, Cortes A, Lluis C, Canela EI, Casado V, McCormick PJ, Ferre S, Functional Selectivity of Allosteric Interactions within G Protein-Coupled Receptor Oligomers: The Dopamine D1-D3 Receptor Heterotetramer, Mol. Pharmacol. 86 (2014) 417–429. doi:10.1124/mol.114.093096. [PubMed: 25097189]

[42]. Ferré S, Ciruela F, Casadó V, Pardo L, Oligomerization of G protein-coupled receptors: Still doubted?, in: Prog. Mol. Biol. Transl. Sci, Elsevier B.V., 2020: pp. 297–321. doi:10.1016/bs.pmbts.2019.11.006.

[43]. Casadó-Anguera V, Cortés A, Casadó V, Moreno E, Targeting the receptor-based interactome of the dopamine D1 receptor: looking for heteromer-selective drugs., Expert Opin. Drug Discov. 14 (2019) 1297–1312. doi:10.1080/17460441.2019.1664469. [PubMed: 31507210]

[44]. Moreland RB, Patel M, Hsieh GC, Wetter JM, Marsh K, Brioni JD, A-412997 is a selective dopamine D4 receptor agonist in rats, Pharmacol. Biochem. Behav. 82 (2005) 140–147. doi:10.1016/j.pbb.2005.08.001. [PubMed: 16153699]

[45]. Good CH, Wang H, Chen YH, Mejias-Aponte CA, Hoffman AF, Lupica CR, Dopamine D4 receptor excitation of lateral habenula neurons via multiple cellular mechanisms, J. Neurosci. 33 (2013) 16853–16864. doi:10.1523/JNEUROSCI.1844-13.2013. [PubMed: 24155292]

[46]. Furth KE, McCoy AJ, Dodge C, Walters JR, Buonanno A, Delaville C, Neuronal correlates of ketamine and walking induced gamma oscillations in the medial prefrontal cortex and mediodorsal thalamus, PLoS One. 12 (2017) e0186732. doi:10.1371/journal.pone.0186732. [PubMed: 29095852]

[47]. Pihlavisto M, Scheinin M, Functional assessment of recombinant human α2-adrenoceptor subtypes with Cytosensor microphysiometry, Eur. J. Pharmacol. 385 (1999) 247–253. doi:10.1016/S0014-2999(99)00715-3. [PubMed: 10607883]

[48]. Hoeren M, Brawek B, Mantovani M, Löffler M, Steffens M, Van Velthoven V, Feuerstein TJ, Partial agonism at the human α2A-autoreceptor: Role of binding duration, Naunyn. Schmiedebergs. Arch. Pharmacol. 378 (2008) 17–26. doi:10.1007/s00210-008-0295-6. [PubMed: 18496673]

[49]. Gonzalez-Maeso J, Meana J, Heterotrimeric G Proteins: Insights into the Neurobiology of Mood Disorders, Curr. Neuropharmacol 4 (2006) 127–138. doi:10.2174/157015906776359586. [PubMed: 18615130]

[50]. Söderberg O, Leuchowius K-J, Gullberg M, Jarvius M, Weibrecht I, Larsson L-G, Landegren U, Characterizing proteins and their interactions in cells and tissues using the in situ proximity ligation assay, Methods. 45 (2008) 227–232. doi:10.1016/j.ymeth.2008.06.014. [PubMed: 18620061]

[51]. Rivera-Oliver M, Moreno E, Álvarez-Bagnarol Y, Ayala-Santiago C, Cruz-Reyes N, Molina-Castro GC, Clemens S, Canela EI, Ferré S, Casadó V, Díaz-Ríos M, Adenosine A1-Dopamine D1 Receptor Heteromers Control the Excitability of the Spinal Motoneuron, Mol. Neurobiol. 56 (2019) 797–811. doi:10.1007/s12035-018-1120-y. [PubMed: 29797183]

[52]. Navarro G, Cordomí A, Casadó-Anguera V, Moreno E, Cai N-S, Cortés A, Canela EI, Dessauer CW, Casadó V, Pardo L, Lluís C, Ferré S, Evidence for functional pre-coupled complexes of receptor heteromers and adenylyl cyclase., Nat. Commun. 9 (2018) 1242. doi:10.1038/s41467-018-03522-3. [PubMed: 29593213]

[53]. Cai N-S, Quiroz C, Bonaventura J, Bonifazi A, Cole TO, Purks J, Billing AS, Massey E, Wagner M, Wish ED, Guitart X, Rea W, Lam S, Moreno E, Casadó-Anguera V, Greenblatt AD, Jacobson AE, Rice KC, Casadó V, Newman AH, Winkelman JW, Michaelides M, Weintraub E, Volkow

ND, Belcher AM, Ferré S, Opioid–galanin receptor heteromers mediate the dopaminergic effects of opioids, J. Clin. Invest. 130 (2019). doi:10.1172/JCI126912.

[54]. Guitart X, Moreno E, Rea W, Sánchez-Soto M, Cai N-S, Quiroz C, Kumar V, Bourque L, Cortés A, Canela EI, Bishop C, Newman AH, Casadó V, Ferré S, Biased G Protein-Independent Signaling of Dopamine D1-D3 Receptor Heteromers in the Nucleus Accumbens, Mol. Neurobiol. (2019) 1–14. doi:10.1007/s12035-019-1564-8.

[55]. Köfalvi A, Moreno E, Cordomí A, Cai NS, Fernández-Dueñas V, Ferreira SG, Guixà-González R, Sánchez-Soto M, Yano H, Casadó-Anguera V, Cunha RA, Sebastião AM, Ciruela F, Pardo L, Casadó V, Ferré S, Control of glutamate release by complexes of adenosine and cannabinoid receptors, BMC Biol. 18 (2020). doi:10.1186/s12915-020-0739-0.

[56]. Violin JD, Lefkowitz RJ, β-Arrestin-biased ligands at seven-transmembrane receptors, Trends Pharmacol. Sci. 28 (2007) 416–422. doi:10.1016/j.tips.2007.06.006. [PubMed: 17644195]

[57]. Yano H, Cai NS, Xu M, Verma RK, Rea W, Hoffman AF, Shi L, Javitch JA, Bonci A, Ferré S, Gs- versus Golf-dependent functional selectivity mediated by the dopamine D1 receptor, Nat. Commun. 9 (2018). doi:10.1038/s41467-017-02606-w.

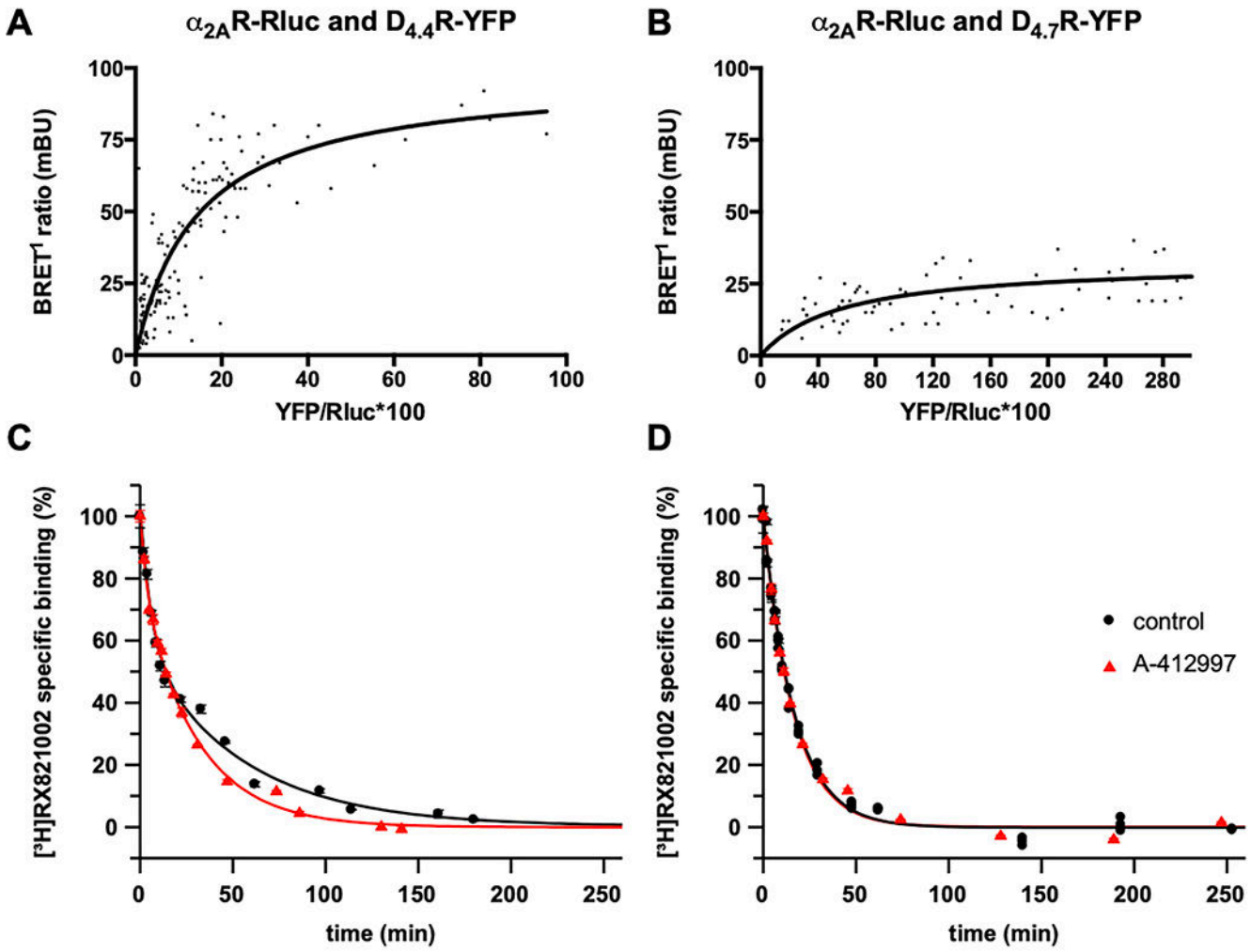


**Fig. 1. $D_{4.4}$R and $D_{4.7}$R heteromerize with $\alpha_{2A}$R in HEK-293T cells.**

(**A** and **B**) BRET saturation experiments were performed using HEK-293T cells transiently transfected with $\alpha_{2A}$R-RLuc cDNA (0.55 μg) and increasing concentrations of (**A**) $D_{4.4}$R-YFP cDNA (0.2-3 μg) or (**B**) $D_{4.7}$R-YFP cDNA (0.2-3.5 μg). Curves were obtained from 3-8 different experiments. mBU: milli BRET units. (**C** and **D**) Radioligand dissociation curves of [$^3$H]RX821002 in the absence (black curve) or presence (red curve) of the selective $D_4$R agonist A-412997 were performed in membrane preparations from tetracycline-inducible HEK-293T cells expressing $D_{4.4}$R (**C**) or $D_{4.7}$R (**D**) and transiently transfected with $\alpha_{2A}$R. Data were fit by the dissociation equation (6) that appears in the materials and methods section. Values are means ± SEM from a representative experiment of 4 different experiments performed in triplicate (see Table 1 for kinetic constant values and statistical comparisons).

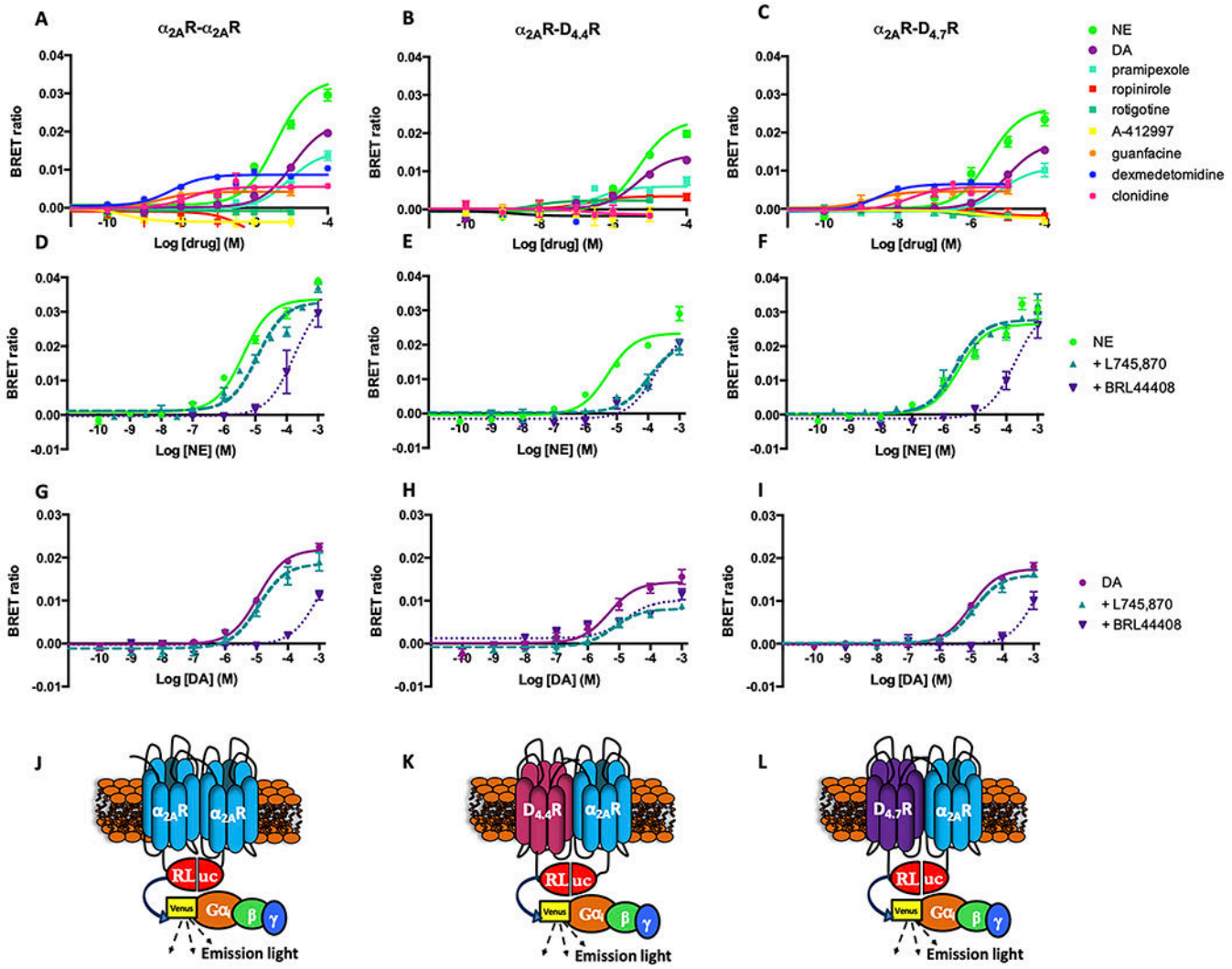


**Fig. 2. Ligand-induced changes in the interaction between $G\alpha_{i1}$ protein and $\alpha_{2A}$R-$\alpha_{2A}$R homomers, $\alpha_{2A}$R-$D_{4.4}$R heteromers and $\alpha_{2A}$R-$D_{4.7}$R heteromers.**

CODA-RET experiments in HEK-293T cells co-transfected with $\alpha_{2A}$R fused to the C-terminus of RLuc and $\alpha_{2A}$R (**A, D, G, J**), $D_{4.4}$R (**B, E, H, K**) or $D_{4.7}$R (**C, F, I, L**) fused to the N-terminus of RLuc and the $G\alpha_{i1}$ subunit fused to mVenus. Concentration-response experiments of changes in BRET ratio induced by norepinephrine (NE), dopamine (DA), pramipexole, ropinirole, rotigotine, A-412997, guanfacine, dexmedetomidine and clonidine (**A** to **C**). Concentration-response experiments of changes in BRET ratio induced by NE (**D, E, F**) and DA (**G, H, I**) in the presence or absence of the $D_4$R antagonist L745,870 (10 μM) or the $\alpha_2$R antagonist BRL44408 (10 μM). Data represent the mean ± SEM of 3-12 different experiments performed in triplicate (see Table 2 and 3 for $EC_{50}$ and $E_{max}$ values and statistical comparisons). (**J, K, L**) Schematic representations of the CODA-RET assay.

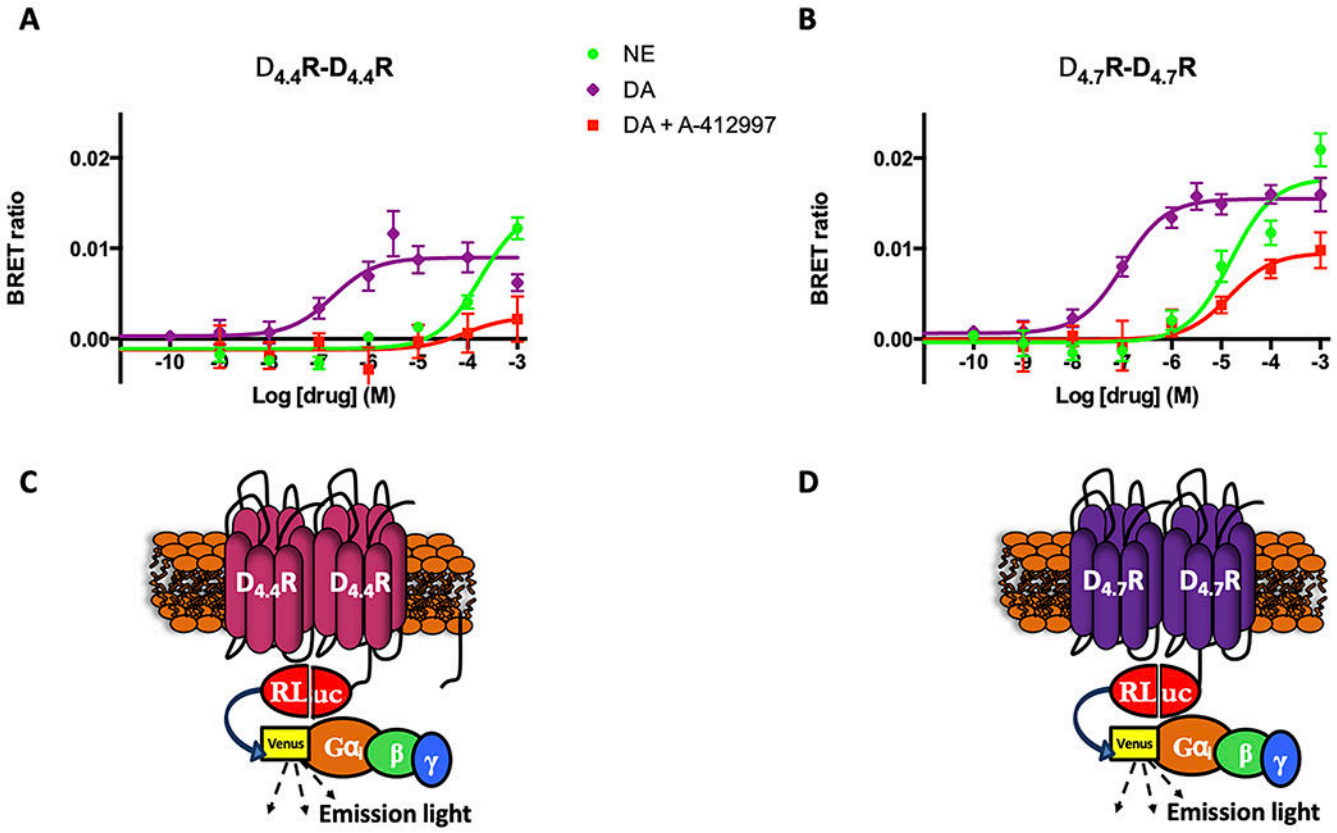


**Fig. 3. Ligand-induced changes in the interaction between $G\alpha_{i1}$ protein and $D_{4.4}R$-$D_{4.4}R$ or $D_{4.7}R$-$D_{4.7}R$ heteromers.**

CODA-RET experiments in HEK-293T cells co-transfected with either $D_{4.4}R$ (**A** and **C**) or $D_{4.7}R$ (**B** and **D**) fused to the C-terminus and N-terminus of RLuc and the $G\alpha_{i1}$ subunit fused to mVenus. Concentration-response experiments of changes in BRET ratio induced by norepinephrine (NE), dopamine (DA) and DA in the presence of the $D_4R$ antagonist A-412997 (1 μM) in the interaction of $D_{4.4}R$-$D_{4.4}R$ (**A**) or $D_{4.7}R$-$D_{4.7}R$ (**B**) dimers with $G\alpha_{i1}$ protein. BRET values are expressed as absolute values and represent the mean ± SEM of 5-14 different experiments performed in triplicate.

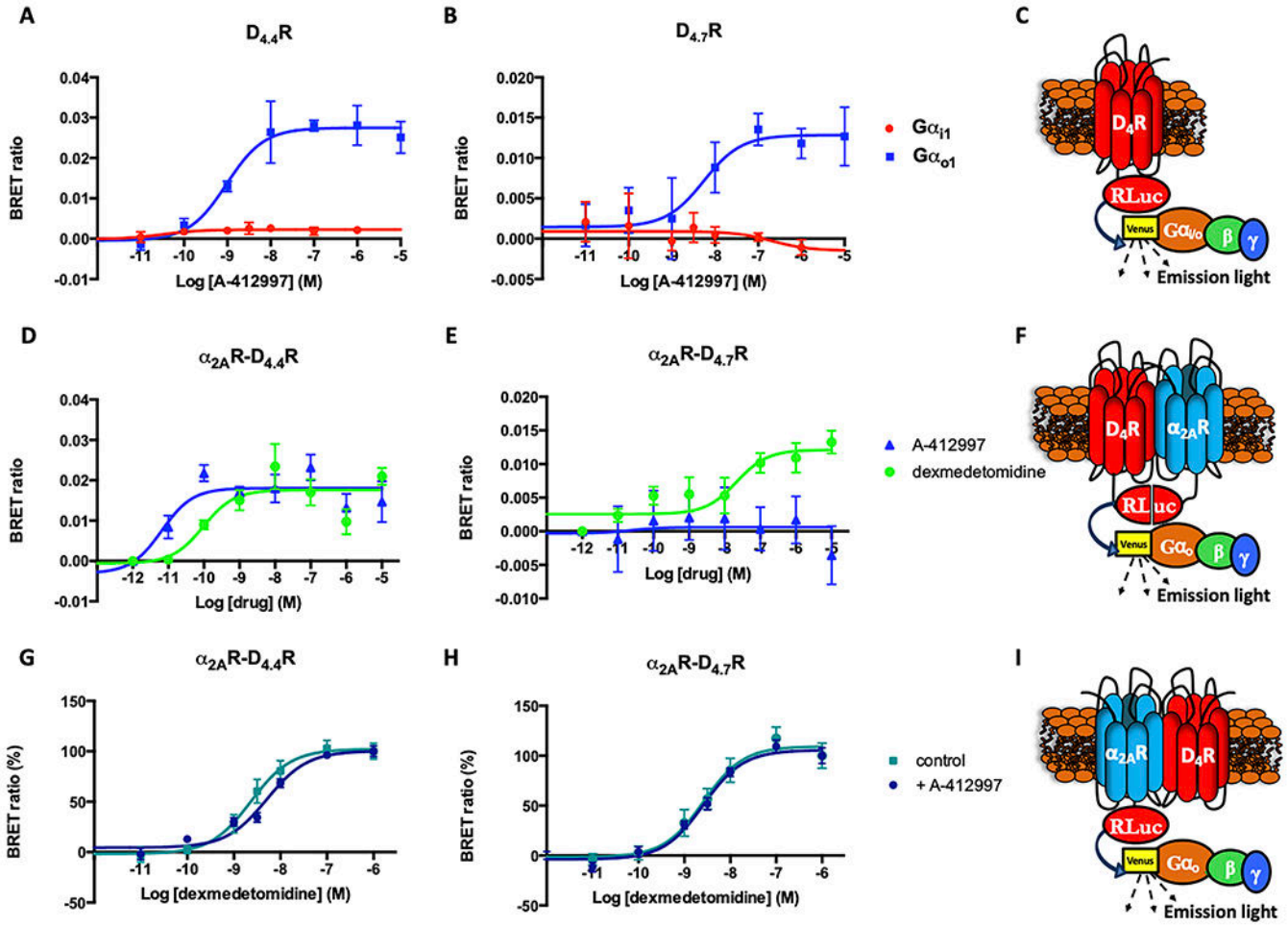


**Fig. 4. Functional selectivity of $\alpha_{2A}$R and $D_4$R ligands dependent on the α subunit of the G protein and the $D_4$R polymorphic variant.**

(**A, B, C**) BRET experiments in HEK-293T cells co-transfected with either $D_{4.4}$R (**A**) or $D_{4.7}$R (**B**) fused to RLuc and $G\alpha_{i1}$ or $G\alpha_{o1}$ subunits fused to mVenus. Concentration-response experiments of changes in BRET ratio induced by the $D_4$R agonist A-412997. (**D, E, F**) CODA-RET experiments in HEK-293T cells co-transfected with $\alpha_{2A}$R fused to the C-terminus of RLuc and $D_{4.4}$R (**D**) or $D_{4.7}$R (**E**) fused to the N-terminus of RLuc and the $G\alpha_{o1}$ subunit fused to mVenus. Concentration-response experiments of changes in BRET ratio induced by A-412997 and the $\alpha_{2A}$R agonist dexmedetomidine. (**G, H, I**) BRET experiments in HEK-293T cells co-transfected with $\alpha_{2A}$R fused to RLuc and unfused $D_{4.4}$R (**G**) or $D_{4.7}$R (**H**) and the $G\alpha_{o1}$ subunit fused to mVenus. Concentration-response experiments of changes in BRET ratio induced by dexmedetomidine with and without A-412997. BRET values are expressed in absolute values (**A, B, D, E**) or as the percentage of the maximal effect of dexmedetomidine alone (**G** and **H**) and represent the mean ± SEM of 5-8 different experiments performed in triplicate. (**C, F, I**) Schematic representations of the different BRET assays.

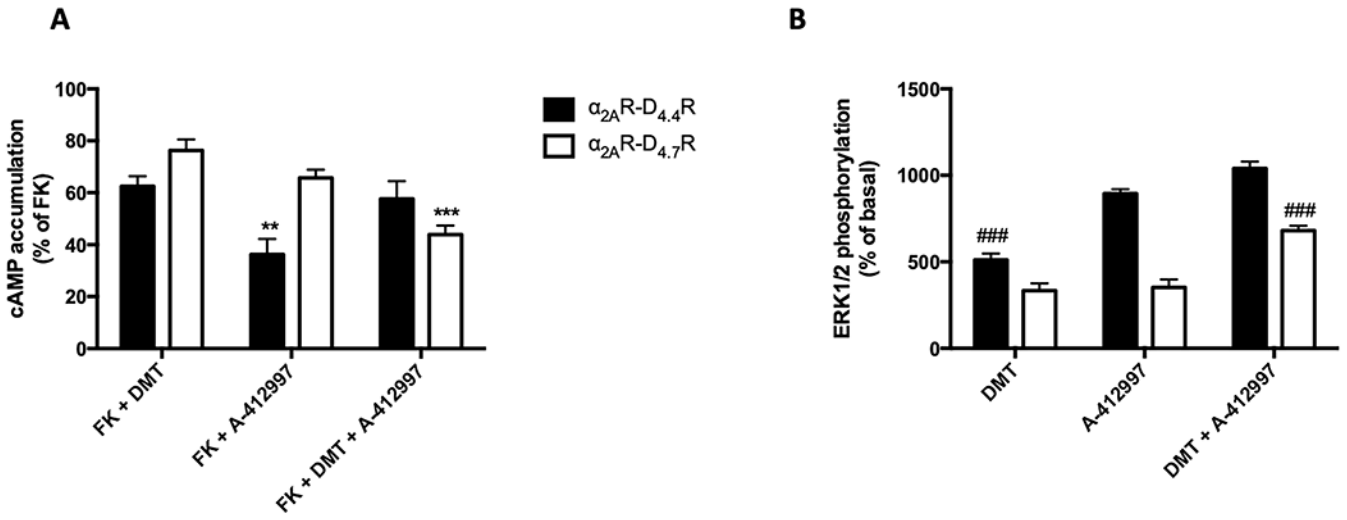


**Fig. 5. Differential signaling in $\alpha_{2A}$R-$D_{4.4}$R and $\alpha_{2A}$R-$D_{4.7}$R cells.**

Agonist-induced adenylyl cyclase inhibition and ERK1/2 phosphorylation assays in tetracycline-inducible HEK-293T cells expressing $D_{4.4}$R (black bars) or $D_{4.7}$R (white bars) and transiently transfected with $\alpha_{2A}$R. (**A**) For cAMP determination, cells were treated with the $\alpha_{2A}$R agonist dexmedetomidine (DMT, 100 nM), the $D_4$R agonist of A-412997 (100 nM) or both agonists in the presence of forskolin (FK, 0.5 μM). Values are expressed as means ± SEM of the percentage of cAMP concentration relative to the effect of FK alone of 7 independent experiments performed in triplicates. (**B**) For ERK1/2 phosphorylation assays, cells were treated with DMT (300 nM), A-412997 (300 nM) or both agonists. Values are expressed as means ± SEM of the percentage of phosphorylation relative to basal levels in not treated cells of 5-7 independent experiments performed in triplicates. Representative western-blots are shown in fig. S4. ** $p < 0.01$, *** $p < 0.001$ *versus* DMT treatment; ### $p < 0.001$ *versus* A-412997 treatment (two-way ANOVA followed by Tuckey's *post hoc* test).

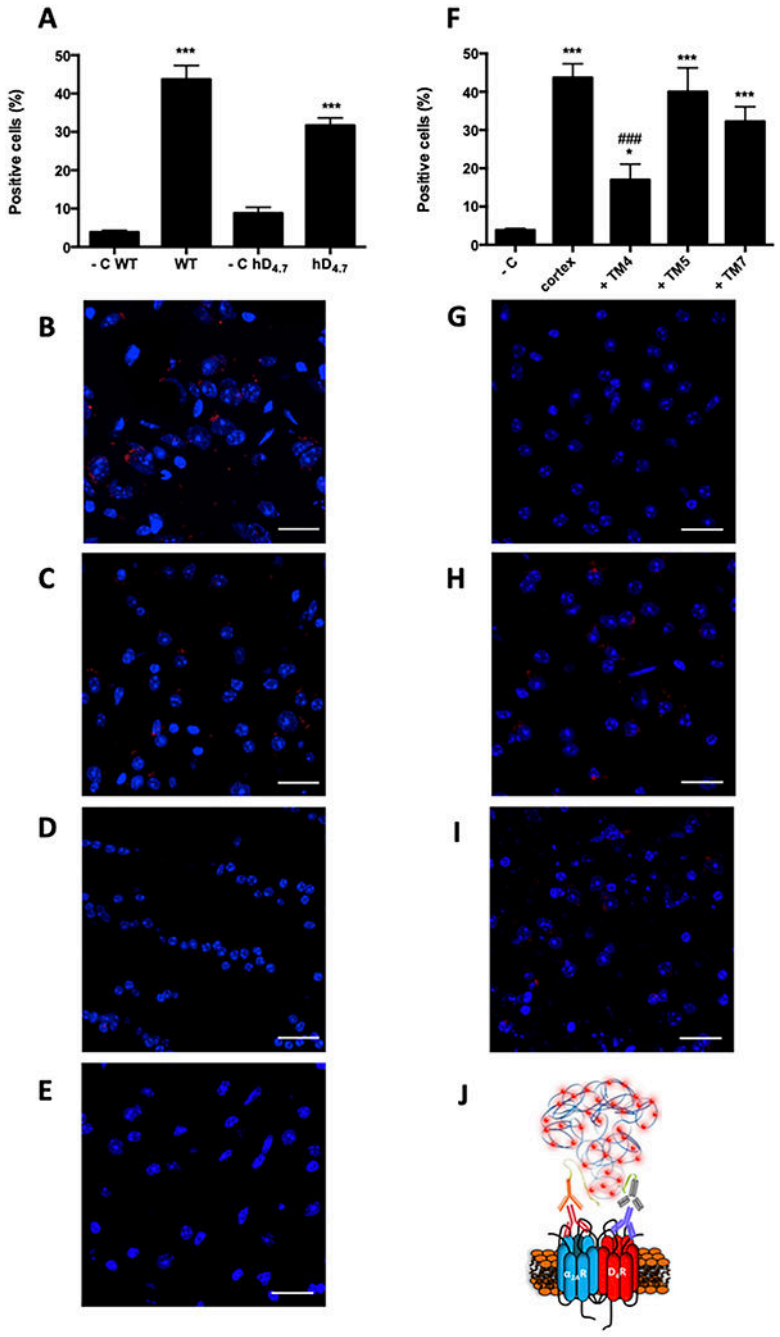


**Fig. 6. Expression of $\alpha_{2A}$R-$D_4$R heteromers in cortical tissue from WT and knock-in $hD_{4.7}$R mice.**

(**A**) Quantification of cells showing $\alpha_{2A}$R-$D_4$R complexes with the PLA assay from cortical brain slices of WT and knock-in $hD_{4.7}$R mice. Representative confocal microscopy images from cortex of WT (**B**) or knock-in $hD_{4.7}$R (**C**) mice, from corpus callosum of WT mice (**D**) or from cortex of WT mice in which primary antibody against $\alpha_{2A}$R is missing (**E**) (superimposed sections). (**F**) Quantification of cells showing $\alpha_{2A}$R-$D_4$R complexes with the PLA assay from cortical brain slices of WT mice in the absence or presence of TM peptides

of the $D_4R$ (TM4, TM5 and TM6). Representative confocal microscopy images from cortex of WT in the presence of $D_4R$ TM4 (**G)**, TM5 (**H**) or TM7 (**I**) (superimposed sections). (**J**) Schematic representation of the PLA assay. The $\alpha_{2A}R$-$D_4R$ complexes appear as red spots. Cell nuclei are stained with DAPI (blue). Scale bars = 20 μm. Cortical slices were treated for 4 h with vehicle or with 4 μM of the corresponding TM peptide before performing the PLA assay. The number of positive cells (containing one or more red spots) is expressed as the percentage of the total number of cells (% of positive cells) and data represent the mean ± SEM of counts in 4–8 different fields of 3 different experiments. * $p < 0.05$, *** $p < 0.001$ *versus* the respective negative control in the corpus callosum (- C); ### $p < 0.001$ *versus* cortex WT, Student's *t* test (**A**); one-way ANOVA followed by Dunnett's *post hoc* test) (**F**).

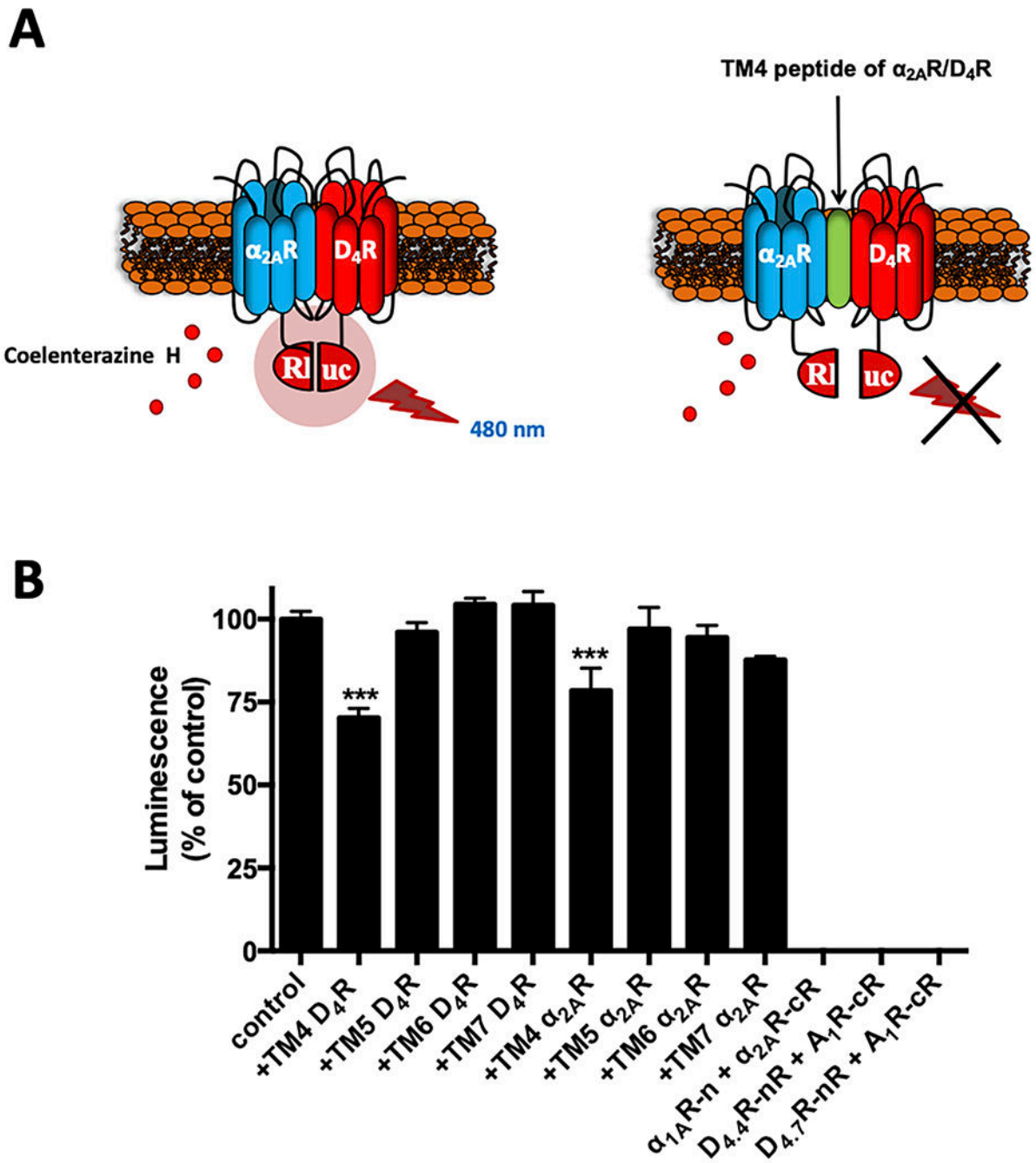


**Fig. 7. Disturbing effect of TM peptides on $\alpha_{2A}$R-$D_4$R heteromerization in bimolecular luminescence complementation experiments.**

**(A)** Schematic representation of the effect of transmembrane peptides disturbing $\alpha_{2A}$R-$D_4$R heteromerization and, therefore, RLuc reconstitution of bimolecular luminescence complementation. (**B**) Quantification of luminescence due to RLuc complementation in HEK-293 cells co-expressing $D_{4.4}$R-nRLuc and $\alpha_{2A}$R-cRLuc in the absence or presence of TM4, TM5, TM6 and TM7 peptides of $\alpha_{2A}$R and $D_4$R. Cells were treated for 4 h with vehicle or with the corresponding TM peptide (2 μM) before performing the

complementation assay. Values (in % of control) represent means ± SEM from 5–10 different experiments performed in triplicate. Control luminescence was 1,000,000±100,000 arbitrary units. Negative controls were obtained with the pairs $\alpha_{1A}$R-nRLuc and $\alpha_{2A}$R-cRLuc or $D_4$R-nRLuc and $A_1$R-cRLuc, which showed luminescence values lower than 1% of control. Statistical significance was calculated by one-way ANOVA followed by Dunnett's *post hoc* test. *** $p < 0.001$ *versus* cells non-treated with the corresponding TM.

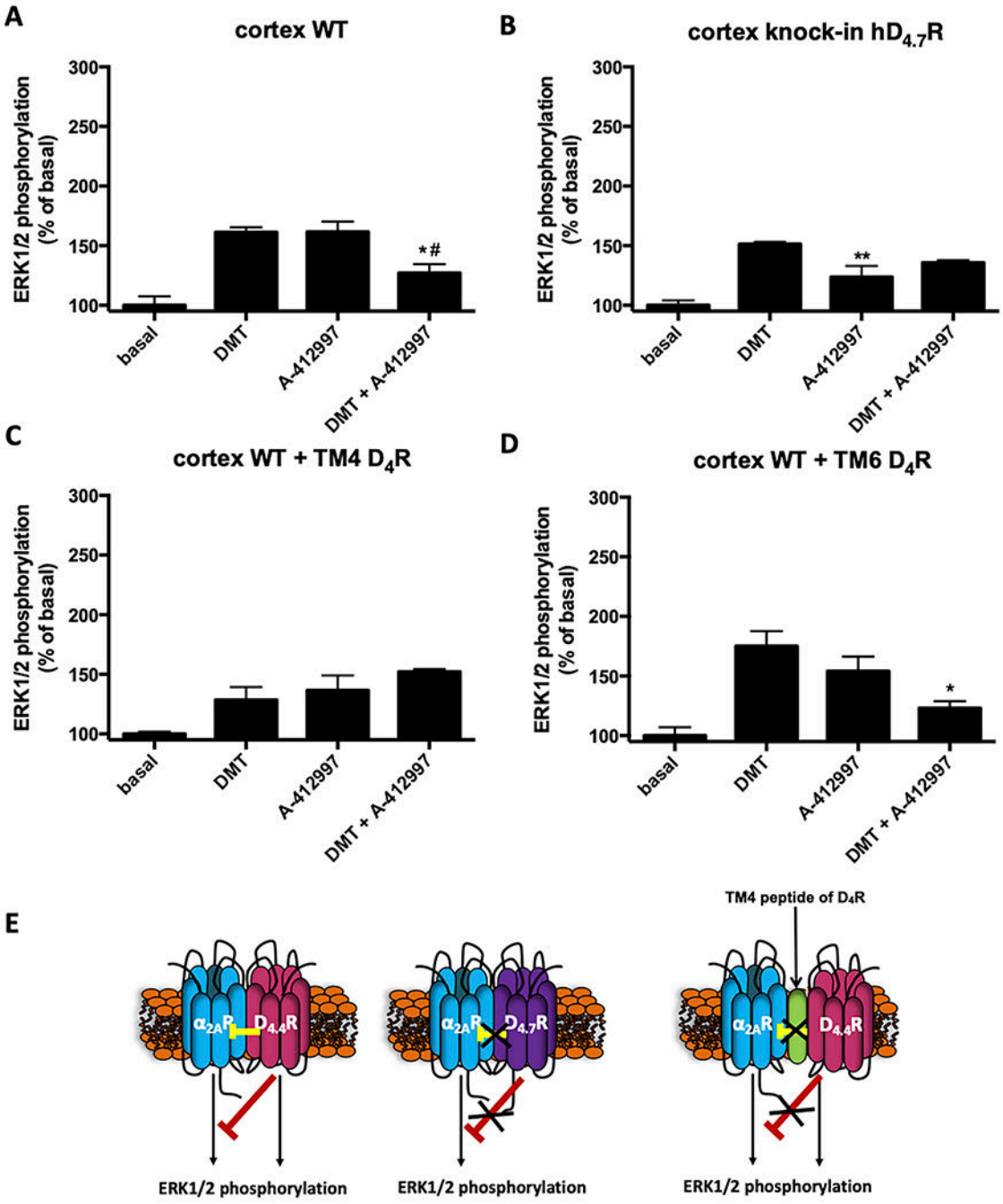


**Fig. 8. Differential signaling of $\alpha_2$R-$D_4$R heteromers expressed in cortical tissue from WT and knock-in $hD_{4.7}$R mice.**

ERK1/2 phosphorylation in cortical brain slices from WT (**A, C, D**) and knock-in $hD_{4.7}$R (**B**) mice determined by western-blot. Cortical slices were treated for 4 h with vehicle (**A** and **B**) or with 4 the $D_4$R interference peptides TM4 (**C**) or TM6 (**D**) (4 μM in both cases) before treatment with the $\alpha_2$R agonist dexmedetomidine (DMT, 1 μM), the $D_4$R agonist A-412997 (1 μM) or both agonists. Values are expressed as mean ± SEM of phosphorylation relative to basal levels in not treated slices of 3–5 independent experiments performed in quadruplicate.

Representative western-blots are shown in fig. S4. * $p < 0.05$, ** $p < 0.01$ *versus* 1 μM DMT; # $p < 0.05$ *versus* 1 μM A-412997 (one-way ANOVA followed by Bonferroni's post hoc test). (**E**) Schematic representation of the allosteric interactions within the $\alpha_{2A}$R-$D_4$R heteromers and the effect of transmembrane peptide TM4 of both receptors disturbing the heteromer formation and, therefore, the inter-protomer allosteric modulations in WT mice.

**Table 1.**

**Effect of a $D_4R$ agonist on dissociation kinetic parameters of the $\alpha_{2A}R$ radiolabeled antagonist.**

Dissociation kinetic assays were performed at 12°C on membranes from HEK-293T cells expressing $D_{4.4}R$ or $D_{4.7}R$ and $\alpha_{2A}R$ receptors. $k_{off}$ values are means ± SEM from four different experiments performed in triplicate fitted with the dissociation equation (6) (see Materials and Methods section).

| | $\alpha_{2A}R$-$D_{4.4}R$ | | | | $\alpha_{2A}R$-$D_{4.7}R$ | |
|---|---|---|---|---|---|---|
| | $k_{off1}$ ($min^{-1}$) | $RT_1$ (min)[a] | $k_{off2}$ ($min^{-1}$) | $RT_2$ (min)[a] | $k_{off}$ ($min^{-1}$) | RT (min)[a] |
| Control | 0.14±0.03 | 7 | 0.020±0.004 | 50 | 0.058±0.002 | 17 |
| + A-412997 | 0.25±0.07* | 4 | 0.036±0.007* | 28 | 0.060±0.007 | 17 |

*$p < 0.05$ *versus* the parameters obtained in the absence of A-412997 (Student's *t*-test).

[a]RT: residence time.

**Table 2.**

**Ligand-induced changes in the interaction between $G\alpha_{i1}$ protein and $\alpha_{2A}R$-$\alpha_{2A}R$, $\alpha_{2A}R$-$D_{4.4}R$ and $\alpha_{2A}R$-$D_{4.7}R$ dimers.**

Experiments were performed in HEK-293T cells transiently expressing $\alpha_{2A}R$-cRLuc and $\alpha_{2A}R$-nRLuc, $\alpha_{2A}R$-cRLuc and $D_{4.4}R$-nRLuc or $\alpha_{2A}R$-cRLuc and $D_{4.7}R$-nRLuc, the G protein subunits $G\alpha_{i1}$-YFP and unfused $\beta_1$ and $\gamma_2$. $EC_{50}$ is expressed as mean ± SEM and $E_{max}$ as mean ± SEM in % of NE of 5-12 different experiments performed in triplicate.

| | $\alpha_{2A}R$-$\alpha_{2A}R$ | | $\alpha_{2A}R$-$D_{4.4}R$ | | $\alpha_{2A}R$-$D_{4.7}R$ | |
|---|---|---|---|---|---|---|
| | **$EC_{50}$ (μM)** | **$E_{max}$** | **$EC_{50}$ (μM)** | **$E_{max}$** | **$EC_{50}$ (μM)** | **$E_{max}$** |
| NE | 6±1 | 100±3 | 10±3 | 100±5 | 1.9±0.5* | 100±5 |
| DA | 12±1 | 69±2* | 7±2 | 59±4 | 11±2 | 73±2** |
| Pramipexole | 9±2*** | 46±2* | 0.5±0.3 | 28±3 | 5.8±0.6* | 48±5** |
| Ropinirole | - | 0 | 0.4±0.2 | 14±2 | - | 0 |
| Rotigotine | - | 0 | 0.007±0.005 | 13±2 | - | 0 |
| A-412997 | - | 0 | - | 0 | - | 0 |
| Guanfacine | 0.008±0.005 | 14±2 | - | 0 | 0.014±0.011 | 20±3 |
| Dexmedetomidine | 0.011±0.006 | 26±3 | - | 0 | 0.003±0.001 | 30±1 |
| Clonidine | 0.034±0.023 | 18±2 | - | 0 | 0.041±0.013 | 26±4 |

* $p < 0.05$,

** $p < 0.01$,

*** $p < 0.001$ *versus* $\alpha_{2A}R$-$D_{4.4}R$ (one-way ANOVA followed by Tuckey's multiple comparison test).

**Table 3.**

**Effect of the antagonists L745,870 or BRL44408 on NE and DA-induced changes in the interaction between $G\alpha_{i1}$ protein and $\alpha_{2A}R$-$\alpha_{2A}R$, $\alpha_{2A}R$-$D_{4.4}R$ and $\alpha_{2A}R$-$D_{4.7}R$ dimers.**

Experiments were performed in HEK-293T cells transiently expressing $\alpha_{2A}R$-cRLuc and $\alpha_{2A}R$-nRLuc, $\alpha_{2A}R$-cRLuc and $D_{4.4}R$-nRLuc or $\alpha_{2A}R$-cRLuc and $D_{4.7}R$-nRLuc, the G protein subunits $G\alpha_{i1}$-YFP and unfused $\beta_1$ and $\gamma_2$. $EC_{50}$ is expressed as mean ± SEM and $E_{max}$ as mean ± SEM in % of NE or DA of 3-12 different experiments performed in triplicate.

| | $\alpha_{2A}R$-$\alpha_{2A}R$ | | $\alpha_{2A}R$-$D_{4.4}R$ | | $\alpha_{2A}R$-$D_{4.7}R$ | |
|---|---|---|---|---|---|---|
| | **$EC_{50}$ (μM)** | **$E_{max}$ (%)** | **$EC_{50}$ (μM)** | **$E_{max}$ (%)** | **$EC_{50}$ (μM)** | **$E_{max}$ (%)** |
| NE | 6±1 | 100±3 | 10±3 | 100±5 | 1.9±0.5 | 100±5 |
| NE + L745,870 | 13±3 | 96±3 | 130±40 *** | 86±7 | 2.6±0.5 | 118±6 |
| NE +BRL44408 | 330±190 *** | 113±9 | 160±20 *** | 105±10 | 190±30 *** | 125±15 |
| DA | 12±1 | 100±3 | 7±1.5 | 100±6 | 11±2 | 100±3 |
| DA + L745,870 | 11±2 | 90±10 | 8±3 | 61±5 ** | 13±1 | 90±5 |
| DA +BRL44408 | > 1000 *** | 95±5 | 40±20 * | 67±8 ** | > 1000 *** | 120±10 |

* $p < 0.05$,

** $p < 0.01$,

*** $p < 0.001$ *versus* the corresponding cells not treated with antagonists (one-way ANOVA followed by Dunnett's *post hoc* test).